

Resonant Microstructures as Dirac-type Actuators for Acoustic Wave Control

Arpan Mukherjee* and Mourad Sini[†]

May 26, 2026

Abstract

We study interior control of the acoustic wave equation via effective point sources generated by a finite cluster of resonant perturbations (modeling acoustic subwavelength bubbles). At the abstract level, after localizing the whole-space dynamics to a large auxiliary observation domain, we consider a Dirichlet spectral formulation of the wave equation with finitely many point actuators located at prescribed interior points. Restricting to a finite spectral band of Dirichlet eigenfrequencies, we prove that, under a natural full-rank condition on the associated coupling matrix, arbitrary trajectories on the corresponding spectral subspace can be realized, with quantitative bounds on the control cost in terms of spectral-band geometry and actuator placement.

We then show that these ideal actuators can be realized by clusters of small, high-contrast bubbles. Using a time-domain asymptotic expansion, the scattered field is represented as a superposition of retarded monopoles whose amplitudes satisfy a finite-dimensional delayed hyperbolic system. In the Laplace domain, this induces a transfer operator whose pole structure encodes the Minnaert resonance with a collective attenuation.

We prove that the associated actuator map is ill-conditioned away from resonance, whereas, under a cluster-level transducer accessibility condition linking the incident fields to the dominant cluster channels, it admits a bounded right inverse on suitable Minnaert bands. Consequently, one obtains spectral tracking of the wave field with error $\mathcal{O}(\varepsilon^\gamma)$ as the bubble size $\varepsilon \rightarrow 0$.

Keywords. Wave equation, Dirac actuators, Trajectory tracking control, Resonant perturbations, Kato's analytic perturbation, Perron-Frobenius spectrum, Minnaert resonances, Actuation map, Toeplitz matrix.

Contents

| | | |
|----------|--|----------|
| 1 | Introduction | 2 |
| 1.1 | Control of wave equations with localised and structured actuators | 2 |
| 1.2 | Resonant bubbles and asymptotic models | 2 |
| 1.3 | Main steps of the construction | 3 |
| 2 | Mathematical Formulation and Main Results | 4 |
| 2.1 | Geometric and Functional Setting | 4 |
| 2.2 | Mathematical Formulation: From Ideal Control to Bubble-Based Realisation | 5 |
| 2.3 | Dual-Scale Geometry and Asymptotics | 6 |
| 2.4 | Spectral Isolation and Generic Controllability | 10 |
| 2.5 | Quantitative Estimation of the Intra-Cluster Spectral Gap | 12 |
| 2.6 | Control Objective and Main Results | 13 |

*MSU-BIT SMBU Joint Research Center of Applied Mathematics, Shenzhen MSU-BIT University, Shenzhen, People's Republic of China (arpan.mukherjee@smbu.edu.cn and arpanmath99@alumni.iitm.ac.in).

[†]Radon institute, RICAM, Austrian Academy of Sciences, Altenbergerstrasse 69, 4040 Linz, Austria (mourad.sini@oeaw.ac.at). The work of M. Sini is partially supported by the Austrian Science Fund (FWF): P 32660 and P: 36942.

| | | |
|----------|---|-----------|
| 3 | Ideal Point-Actuator Tracking | 15 |
| 3.1 | Abstract formulation and well-posedness | 15 |
| 3.2 | Tracking on a finite spectral subspace | 17 |
| 4 | Bubble Dynamics and the Transfer Matrix | 18 |
| 4.1 | Scattered field as a superposition of retarded monopoles | 18 |
| 4.2 | Cluster reduction and localization to the bounded domain Ω | 20 |
| 4.3 | Laplace-domain transfer function of the bubble subsystem | 21 |
| 5 | Pole Structure and the Minnaert Resonance: Proof of Proposition 2.1 | 22 |
| 5.1 | Proof of Proposition 2.1(1): Meromorphic structure of the transfer matrix | 22 |
| 5.2 | Proof of Proposition 2.1(2): Discrete Poles and Asymptotic Cluster Separation | 23 |
| 5.3 | Proof of Proposition 2.1(3): Residue Expansion at the Distinguished Pole | 28 |
| 6 | Resonant Gain and Approximate Surjectivity | 28 |
| 6.1 | The Actuator Map and Band-Pass Filtering | 28 |
| 6.2 | Asymptotic Divergence and Control Constraints on Non-Resonant Bands | 29 |
| 6.3 | Approximate Surjectivity on the Minnaert Band | 30 |
| 7 | Energy Estimates and Proof of the Main Result | 33 |

1 Introduction

1.1 Control of wave equations with localised and structured actuators

The control and observation of wave equations is a classical topic with an extensive literature on boundary control, distributed control, observability, and stabilisation (see, e.g., [6, 14, 17, 22, 24]). In many of these works, controls act either on a portion of the boundary or on a nontrivial subregion, and well-posedness and controllability are typically expressed via geometric conditions (such as the geometric control condition) and microlocal propagation properties.

By contrast, *point* or *highly localised* interior actuators lead to more delicate issues: PDE-control coupling is concentrated at a finite set of points, natural energy spaces interact with singular source terms, and available control directions are strongly constrained (see, e.g., [22, 23]). Related finite-dimensional actuator mechanisms, including distributional and actuator-based feedback constructions, have been studied for parabolic systems [13, 20]. In applications, such actuators can be realised by physical devices with their own internal dynamics, entering the PDE only through the output of a finite-dimensional subsystem (e.g., plasmonic heat generation [20]).

The present work fits naturally in this latter perspective with an additional physical layer. The underlying time-domain scattering problem is posed in the full space \mathbb{R}^3 : an incident acoustic field (e.g., from exterior transducers) interacts with a finite cluster of small resonant bubbles. Away from the bubbles, the resulting wave field is approximated by an effective superposition of retarded monopoles. We introduce a bounded and smooth domain Ω as a large observation and computational domain containing the bubble cluster. For each fixed time horizon $T > 0$, it is chosen sufficiently large so that, by finite propagation speed, waves generated in the active region do not interact with $\partial\Omega$ during the time interval. A Dirichlet spectral decomposition on Ω is therefore used as a localized finite-dimensional coordinate system for the tracking problem.

1.2 Resonant bubbles and asymptotic models

Resonant bubbles are a well-studied class of high-contrast inhomogeneities. A single immersed gas bubble exhibits a natural volume oscillation frequency—the Minnaert resonance—where its scattering response is dominated by a frequency-sensitive monopole (see, e.g., [2, 3, 4, 5, 7, 15]). In the presence of many bubbles, these monopole modes interact, leading to cluster resonances, subwavelength band gaps, and rich effective-medium behaviour.

Rigorous time-domain asymptotics for such media have been developed in [18, 19]. Under assumptions of high contrast, subwavelength size, and suitable spacing, these works show that the acoustic transmission solution in \mathbb{R}^3 with incident field u^{in} admits, on finite time intervals and *away from the bubbles*, the expansion

$$u^\varepsilon(x, t) = u^{\text{in}}(x, t) + \sum_{i=1}^M \frac{1}{4\pi|x - z_i|} q_i^\varepsilon(t - c_0^{-1}|x - z_i|) + R^\varepsilon(x, t), \quad (1.1)$$

where q_i^ε are scalar amplitudes satisfying a finite-dimensional delayed system driven by the traces $u^{\text{in}}(z_i, \cdot)$, and the remainder R^ε is small (in adapted norms) as the bubble radius $\varepsilon \rightarrow 0$.

1.3 Main steps of the construction

The proposed construction is organized into three levels. The first two map the microscopic bubbly medium to finite cluster outputs, while the third contains the control argument.

Level 1. Microscopic resonant bubble system. The starting point is the M -bubble multiple-scattering system (1.1). This microscopic level is retained since intra-cluster interactions generate the requisite Minnaert poles, frequency shifts, and radiative damping. Thus, the primary unknowns are the microscopic amplitudes

$$\mathbf{q}_{\text{mic}}^\varepsilon(t) = (q_1^\varepsilon(t), \dots, q_M^\varepsilon(t)),$$

solving the delayed algebraic system of the M -bubble approximation.

Level 2. Cluster-output representation. The M bubbles are arranged into N local clusters,

$$M = \sum_{\alpha=1}^N M_\alpha, \quad \{1, \dots, M\} = \bigsqcup_{\alpha=1}^N \mathcal{I}_\alpha,$$

with cluster centers y_α . On observation sets away from the microscopic bubble clusters, the background retarded Green kernel is smooth with respect to the source variable inside each local cluster. Hence the M -term representation (1.1) induces the cluster-level expansion

$$\sum_{i=1}^M \mathcal{W}[q_i^\varepsilon; z_i] = \sum_{\alpha=1}^N \mathcal{W}[Q_\alpha^\varepsilon; y_\alpha] + \mathcal{R}_{\text{cl}}^\varepsilon, \quad (1.2)$$

where \mathcal{W} denotes the retarded monopole operator and

$$Q_\alpha^\varepsilon(t) = (B_{\text{out}} \mathbf{q}_{\text{mic}}^\varepsilon(t))_\alpha := \sum_{i \in \mathcal{I}_\alpha} q_i^\varepsilon(t), \quad \alpha = 1, \dots, N. \quad (1.3)$$

The remainder $\mathcal{R}_{\text{cl}}^\varepsilon$ is controlled by the maximal cluster diameter and by the components of the microscopic response which are not aligned with the dominant coherent cluster mode. Thus Q_α^ε is the macroscopic actuator strength carried by the α -th cluster.

At the macroscopic level, the preceding reduction shows that the physical wave field u^ε contains a dominant point-source contribution p^ε . This component is the leading term generated by the effective monopole outputs of the resonant clusters, so that

$$u^\varepsilon(t, x) = u^{\text{in}}(t, x) + p^\varepsilon(t, x) + \text{remainder}.$$

After localization to a bounded and smooth domain Ω , this component is represented by the Dirichlet point-source model

$$\left(\frac{1}{c_0^2} \partial_{tt} - \Delta \right) p^\varepsilon(t, x) = \sum_{\alpha=1}^N Q_\alpha^\varepsilon(t) \delta_{y_\alpha}, \quad (t, x) \in (0, T) \times \Omega,$$

with homogeneous Dirichlet boundary condition on $\partial\Omega$. Here y_α denotes the center of the α -th cluster, while $Q_\alpha^\varepsilon(t)$ is the effective monopole strength generated by that resonant cluster.

Level 3. Control construction. At the control level we separate the design of an ideal cluster-source profile from its physical realization by the bubbly medium. Let Δ_D denote the Dirichlet Laplacian on Ω with its induced spectral decomposition $(\phi_k, \lambda_k)_{k \in \mathbb{N}}$.

Step 1. Ideal finite-dimensional control. We select a Dirichlet spectral subspace

$$H_M = \text{span}\{\phi_{k_1}, \dots, \phi_{k_{N_M}}\}, \quad \omega_{k_\ell} = c_0 \sqrt{\lambda_{k_\ell}} > 0,$$

in the observation domain Ω . The ideal actuators are the cluster-level source strengths located at the macroscopic centers y_α . Their coupling to the selected modal coordinates is described by

$$C_M(\mathbf{y}) = (\phi_{k_\ell}(y_\alpha))_{1 \leq \ell \leq N_M, 1 \leq \alpha \leq N}. \quad (1.4)$$

The condition $\text{rank } C_M(\mathbf{y}) = N_M$ is the finite-dimensional controllability condition. It yields a right inverse L_M and hence, for a prescribed trajectory in H_M , an ideal cluster-source profile

$$q^{\text{ideal}}(t) = c_0^{-2} L_M(\ddot{p}_r(t) + \Lambda_M p_r(t)),$$

where $\Lambda_M = \text{diag}(\omega_{k_1}^2, \dots, \omega_{k_{N_M}}^2)$ is the diagonal matrix of the squared selected modal frequencies. This step is macroscopic: it constructs the effective source profile that would produce the desired modal tracking.

Step 2. Physical realization by resonant bubble clusters. The second control step realizes the ideal profile through incident waves exciting the bubble clusters. The cluster parameters are chosen so that the separated operational Minnaert bands $I_\alpha(\varepsilon)$ cover the selected Dirichlet modal frequencies:

$$\omega_{k_\ell} \in I_{\alpha(\ell)}(\varepsilon), \quad \ell = 1, \dots, N_M, \quad (1.5)$$

for a suitable assignment $\alpha(\ell) \in \{1, \dots, N\}$. In the basic one-channel-per-mode design, $N = N_M$ and $\alpha(\ell) = \ell$. The matching in (1.5) is a frequency matching: the matrix $C_M(\mathbf{y})$ handles the spatial modal coupling in the ideal problem, whereas the separated Minnaert bands provide efficient resonant realization of the temporal components of q^{ideal} . Finally, the incident waves generated by the transducers must access the N cluster channels used in this realization step. This is encoded by a cluster-level transducer matrix evaluated at the centers y_α ; the detailed construction of the exterior-to-cluster realization map is recorded in Section 2.3.

The outcome is a two-stage tracking strategy. First, at the ideal level, one constructs time-dependent point sources which reproduce exactly any prescribed trajectory in a finite-dimensional spectral subspace of the Dirichlet Laplacian, under a natural rank condition on the cluster locations. Second, these ideal sources are realized, up to a small asymptotic error, by suitable collections of Minnaert-resonant bubbles. In this sense, the resonant microstructure provides a physical implementation of finite-band wave tracking: the control is designed at the spectral level, while its realization is carried out through the resonant response of the bubbles.

2 Mathematical Formulation and Main Results

2.1 Geometric and Functional Setting

We distinguish the *physical* bubble problem, posed in \mathbb{R}^3 , from the *abstract control* problem, posed on a $C^{1,1}$ -smooth bounded observation domain Ω containing the bubble cluster.

The reduction from the whole-space formulation to the bounded-domain control model is restricted to a fixed finite time interval $[0, T]$. The bounded domain Ω serves as an auxiliary localization and control domain: the original bubbly scattering problem is naturally posed in \mathbb{R}^3 , whereas the finite-dimensional control problem is formulated on Ω via the Dirichlet spectral decomposition. We choose

Ω sufficiently large relative to the time horizon T and the active bubble region $D := \bigcup_{i=1}^M D_i$ so that the artificial boundary does not interfere with the wave dynamics relevant to the tracking problem. Specifically, based on the finite propagation speed c_0 , we choose Ω such that

$$\text{dist}(D, \partial\Omega) > c_0 T. \quad (2.1)$$

The homogeneous Dirichlet condition used below is therefore a pure localization device, providing a convenient self-adjoint spectral basis with strictly positive eigenvalues.

We set

$$H := L^2(\Omega), \quad V := H_0^1(\Omega),$$

and define the energy space

$$\mathcal{H} := V \times H, \quad \|(u, v)\|_{\mathcal{H}}^2 := \|\nabla u\|_{L^2(\Omega)}^2 + \frac{1}{c_0^2} \|v\|_{L^2(\Omega)}^2,$$

where $c_0 > 0$ is the background sound speed.

The Dirichlet Laplacian $-\Delta_D$ on Ω is defined by

$$-\Delta_D u := -\Delta u, \quad D(-\Delta_D) := H^2(\Omega) \cap H_0^1(\Omega).$$

It is self-adjoint and strictly positive on H and admits an orthonormal basis of eigenfunctions $\{\phi_k\}_{k \geq 1} \subset D(-\Delta_D)$ with

$$-\Delta_D \phi_k = \lambda_k \phi_k, \quad 0 < \lambda_1 \leq \lambda_2 \leq \dots, \quad \lambda_k \rightarrow \infty.$$

We define

$$\omega_k := c_0 \sqrt{\lambda_k} > 0, \quad k \geq 1,$$

and call ω_k the angular frequencies of the Dirichlet modes.

The ideal point actuators used below are located at the macroscopic cluster centers $y_1, \dots, y_N \in \Omega$. For each α we denote by δ_{y_α} the corresponding Dirac mass. In three space dimensions, point evaluation is not a continuous functional on $H_0^1(\Omega)$, so $\delta_{y_\alpha} \notin V' = H^{-1}(\Omega)$ for $V = H_0^1(\Omega)$. As a consequence, the wave equation with point sources is not well-posed in the standard energy space $\mathcal{H} = H_0^1(\Omega) \times L^2(\Omega)$. In this work we therefore interpret point actuation *only after projection onto a finite-dimensional Dirichlet spectral subspace* (Galerkin viewpoint). Since Dirichlet eigenfunctions are smooth, point evaluation is well-defined on such subspaces: for $\varphi \in H_{N_M} := \text{span}\{\phi_k : k \in K_M\}$ we set $\langle \delta_{y_\alpha} | \varphi \rangle := \varphi(y_\alpha)$.

2.2 Mathematical Formulation: From Ideal Control to Bubble-Based Realisation

In this section, we formalize the tracking problem, defining the ideal point-actuated model, its physical bubble-based realization, and our main theoretical guarantees. The core mechanism is intrinsically spectral-band limited, bridging finite-time pressure tracking with bubble-mediated actuation in the time domain.

Definition 1 (Ideal Point-Actuated Model). *Let $\Omega \subset \mathbb{R}^3$ be a bounded domain and $T > 0$ a terminal time. The ideal model for the controlled pressure field $p(x, t)$ is governed by the Dirichlet spectral wave model:*

$$\begin{cases} \frac{1}{c_0^2} \partial_t^2 p - \Delta p = \sum_{\alpha=1}^N q_\alpha(t) \delta_{y_\alpha} & \text{in } \Omega \times (0, T), \\ p = 0 & \text{on } \partial\Omega \times (0, T), \\ p(\cdot, 0) = 0, \quad \partial_t p(\cdot, 0) = 0. \end{cases} \quad (2.2)$$

where $y_\alpha \in \Omega$ are the macroscopic cluster centres and $\mathbf{q}(t) = (q_1(t), \dots, q_N(t))^\top \in L^2(0, T; \mathbb{R}^N)$ is the vector of cluster-level source strengths.

In accordance with the localization condition (2.1), the dominant effective field in (1.1), i.e. the second term there, satisfies the localized problem (2.2).

Definition 2 (Spectral Band Subspace). Let $\{\lambda_k, \phi_k\}_{k=1}^{\infty}$ be the Dirichlet eigenpairs of $-\Delta$ in Ω , with $\omega_k = c_0\sqrt{\lambda_k}$. For a given finite frequency band $J \subset (0, \infty)$, we define the index set $K_J := \{k : \omega_k \in J\}$ and denote its cardinality by $|K_J|$. The corresponding finite-dimensional spectral subspace and its $L^2(\Omega)$ -orthogonal projector are:

$$H_J := \text{span}\{\phi_k : k \in K_J\}, \quad P_J : L^2(\Omega) \rightarrow H_J. \quad (2.3)$$

Projecting (2.2) onto H_J , the modal coefficients $p_k(t) = \langle p(t, \cdot), \phi_k \rangle$ satisfy the finite-dimensional forced oscillator system:

$$\ddot{p}_k(t) + \omega_k^2 p_k(t) = c_0^2 \sum_{\alpha=1}^N q_{\alpha}(t) \phi_k(y_{\alpha}), \quad \forall k \in K_J. \quad (2.4)$$

Definition 3 (Bubble-Based Transmission Problem and Control Spaces). In the physical realization, the ideal cluster actuators are generated by multiple scattering from a finite family $D = \cup_{i=1}^M D_i$ of small, high-contrast bubbles of size ε , with microscopic centres z_i grouped around the macroscopic cluster centres y_{α} . The acoustic pressure $u(x, t)$ is governed by the following transmission problem:

$$\begin{cases} \kappa^{-1}(x) \partial_t^2 u(x, t) - \text{div}(\rho^{-1}(x) \nabla u(x, t)) = \sum_{m=1}^{M_{\text{tr}}} \lambda_m(t) \delta_{x_m^{\text{tr}}}(x) & \text{in } (\mathbb{R}^3 \setminus \partial D) \times (0, T), \\ u|_+ = u|_- & \text{on } \partial D \times (0, T), \\ \rho_c^{-1} \partial_{\nu} u|_+ = \rho_b^{-1} \partial_{\nu} u|_- & \text{on } \partial D \times (0, T), \\ u(\cdot, 0) = 0, \quad \partial_t u(\cdot, 0) = 0 & \text{in } \mathbb{R}^3, \end{cases} \quad (2.5)$$

where ρ_b, ρ_c and κ_b, κ_c denote the densities and bulk moduli inside and outside the bubbles, respectively.

For exterior transducers located at $\{x_m^{\text{tr}}\}_{m=1}^{M_{\text{tr}}} \subset \mathbb{R}^3 \setminus \bar{\Omega}$, we define the physical control space as

$$U_{\text{tr}} := \{\boldsymbol{\lambda} \in H^2(0, T; \mathbb{R}^{M_{\text{tr}}}) : \boldsymbol{\lambda}(0) = \dot{\boldsymbol{\lambda}}(0) = \mathbf{0}\}. \quad (2.6)$$

Because the incident traces $u^{\text{in}}(z_i, \cdot)$ are linear combinations of delayed signals $\boldsymbol{\lambda}(t - \tau)$, the condition $\boldsymbol{\lambda} \in U_{\text{tr}}$ yields the exact L^2 -regularity required for the temporal forcing $\partial_t^2 u^{\text{in}}(z_i, \cdot)$ in (4.4), confirming that the inputs at the bubble centers are strictly parameterized by the finite-dimensional exterior array.

2.3 Dual-Scale Geometry and Asymptotics

Assumption 1 (Material Parameter Scaling). Let $D := \cup_{i=1}^M D_i$. The bulk modulus κ and mass density ρ are piecewise constant and scale with ε as follows:

$$[\kappa(x), \rho(x)] := \begin{cases} [\kappa_c, \rho_c], & x \in \mathbb{R}^3 \setminus \bar{D}, \\ [\bar{\kappa}_{b_i} \varepsilon^2, \bar{\rho}_{b_i} \varepsilon^2], & x \in D_i, \end{cases} \quad (2.7)$$

where the background parameters (κ_c, ρ_c) and the scaled interior parameters $(\bar{\kappa}_{b_i}, \bar{\rho}_{b_i})$ are strictly positive constants independent of ε . Consequently, the local wave speed $c := \sqrt{\kappa/\rho}$ satisfies $c = \mathcal{O}(1)$ uniformly in \mathbb{R}^3 .

To couple the microscopic state to the localized macroscopic control targets, we impose the following topological and spectral conditions on the bubble configuration.

Assumption 2 (Topological and Spectral Separation). For a given $p \in (0, 1)$ and scale parameter $\varepsilon \ll 1$, let the index set $\mathcal{G} = \{1, \dots, M\}$ of M bubbles be partitioned as $\mathcal{G} = \bigsqcup_{\alpha=1}^N \mathcal{G}_\alpha$. Thus M is the number of microscopic bubbles, whereas N is the number of macroscopic local clusters. We denote $M_\alpha := |\mathcal{G}_\alpha|$, so that $\sum_{\alpha=1}^N M_\alpha = M$. Let $z_i \in \mathbb{R}^3$ denote the center of bubble D_i , and let y_α denote the center of the local cluster \mathcal{G}_α . We assume:

- (i) *Spectral detuning:* There exist physical Minnaert frequencies $\{\omega_{M,\alpha}\}_{\alpha=1}^N \subset \mathbb{R}^+$ such that $\omega_{M,i} = \omega_{M,\alpha}$ for all $i \in \mathcal{G}_\alpha$, with $\omega_{M,\alpha} \neq \omega_{M,\beta}$ for all $\alpha \neq \beta$. This is naturally satisfied due to the explicit formulation $\omega_{M,\alpha} = \sqrt{\frac{2\bar{\kappa}_{b_i,\alpha}}{\rho_c \Lambda_{\partial B_{i,\alpha}}}}$ and by choosing different material properties of the inclusions for each disjoint cluster, where $\Lambda_{\partial B_{i,\alpha}}$ is a geometric constant to be specified later.
- (ii) *Dual-scale geometry:* There exist strictly ε -independent constants $c_1, c_2, D_{\min}, D_{\max} > 0$ such that the pairwise distances $d_{ij} := |z_i - z_j|$ satisfy:

$$d_{ij} \in \begin{cases} [c_1 \varepsilon^p, c_2 \varepsilon^p], & \forall i, j \in \mathcal{G}_\alpha, i \neq j \\ [D_{\min}, D_{\max}], & \forall i \in \mathcal{G}_\alpha, \forall j \in \mathcal{G}_\beta, \alpha \neq \beta. \end{cases} \quad (2.8)$$

The effective number of resonant actuators is therefore N . In the target Minnaert band, each local cluster contributes one principal collective resonant mode spanning a one-dimensional subspace $E_\alpha \subset \mathbb{C}^{M_\alpha}$. The dominant cluster subspace E_{dom} and its associated spectral projection Π_{dom} satisfy

$$E_{\text{dom}} := \bigoplus_{\alpha=1}^N E_\alpha \subset \mathbb{C}^M, \quad \dim E_{\text{dom}} = \text{rank } \Pi_{\text{dom}} = N. \quad (2.9)$$

The rank condition required for control is thus a rank- N condition on the dominant cluster residue, ensuring these N principal directions are independently excitable by the incident fields and observable via the effective source strengths.

Under this structural assumption, the exterior time-domain field admits the asymptotic expansion

$$u(x, t) = u^{\text{in}}(x, t) + p^{\text{eff}, \varepsilon}(x, t) + \text{err}_\varepsilon(x, t), \quad (x, t) \in (\Omega \setminus \bar{D}) \times (0, T), \quad (2.10)$$

where $\text{err}_\varepsilon \rightarrow 0$ asymptotically as $\varepsilon \rightarrow 0$. The effective scattered pressure is modeled as a macroscopic point-source field:

$$p^{\text{eff}, \varepsilon}(x, t) := \sum_{\alpha=1}^N \frac{1}{4\pi|x - y_\alpha|} Q_\alpha^\varepsilon(t - c_0^{-1}|x - y_\alpha|), \quad Q_\alpha^\varepsilon := \sum_{i \in \mathcal{G}_\alpha} q_i^\varepsilon. \quad (2.11)$$

The corresponding microscopic and effective cluster-source spaces are defined as $V_{\text{mic}} := L^2(0, T; \mathbb{R}^M)$ and $V_{\text{cl}} := L^2(0, T; \mathbb{R}^N)$.

The physical realization operator is the time-domain map

$$\mathcal{J}^\varepsilon : U_{\text{tr}} \longrightarrow V_{\text{cl}}, \quad \boldsymbol{\lambda} \longmapsto \mathbf{q}_{\text{cl}}^\varepsilon,$$

where $\mathbf{q}_{\text{cl}}^\varepsilon := (Q_1^\varepsilon, \dots, Q_N^\varepsilon)$ denotes the vector of N cluster-level source strengths. In the Laplace domain, the input-output mapping $\widehat{\mathbf{q}}_{\text{cl}}^\varepsilon(s) = \mathcal{H}_{\text{ext}}^\varepsilon(s) \widehat{\boldsymbol{\lambda}}(s)$ is governed by the exterior-to-cluster transfer matrix $\mathcal{H}_{\text{ext}}^\varepsilon(s) \in \mathbb{C}^{N \times M_{\text{tr}}}$, which admits the physical factorization

$$\mathcal{H}_{\text{ext}}^\varepsilon(s) := B_{\text{out}} H_b(s) G_{\text{tr}}(s). \quad (2.12)$$

Here, the transducer trace matrix $G_{\text{tr}}(s) := (G_s(z_i, x_m^{\text{tr}})) \in \mathbb{C}^{M \times M_{\text{tr}}}$ evaluates the incident fields generated by the transducers via the background Green's kernel $G_s(z, x) = \frac{\rho_c}{4\pi|z-x|} e^{-s|z-x|/c_0}$, yielding the microscopic bubble-center traces

$$\widehat{\mathbf{u}}^{\text{in}}(s) \Big|_{\{z_i\}_{i=1}^M} = G_{\text{tr}}(s) \widehat{\boldsymbol{\lambda}}(s). \quad (2.13)$$

The internal physics of the bubble cluster are captured entirely by the structural factorization of the microscopic transfer matrix $H_b(s)$, which processes these incident traces via:

$$H_b(s) := \mathcal{A}_b \mathcal{K}_{\text{dyn}}(s)^{-1} B(s), \quad \text{where} \quad \mathcal{K}_{\text{dyn}}(s) := I + \mathcal{D}(s)^{-1} s^2 \mathcal{Q}(s). \quad (2.14)$$

In this formulation, $\mathcal{D}(s) = \text{diag}(\omega_{M,i}^{-2} s^2 + 1)_{i=1}^M$, the local input operator $B(s) = \mathcal{D}(s)^{-1} s^2 B^{\text{in}}(s)$ converts the incident traces into the forcing vector, and the delayed physical interaction matrix is defined as $\mathcal{Q}_{ij}(s) = \varepsilon \frac{\tilde{C}_j e^{-s\tau_{ij}}}{4\pi d_{ij}}$ for $i \neq j$. Finally, the cluster-output projection $B_{\text{out}} : \mathbb{C}^M \rightarrow \mathbb{C}^N$ aggregates the resulting microscopic source amplitudes into macroscopic strengths via

$$(B_{\text{out}} \mathbf{q})_\alpha = \sum_{i \in g_\alpha} q_i.$$

The spectral behavior of the physical control problem is fundamentally governed by the singular features of $H_b(s)$, which we formalize in the following proposition.

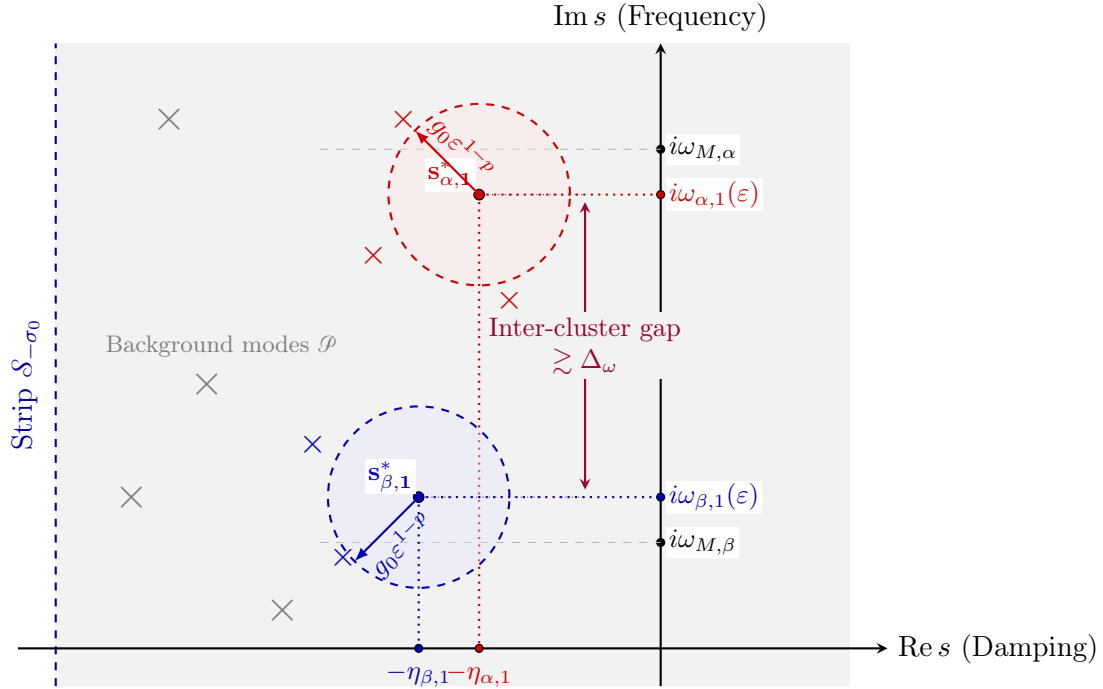


Figure 1: Schematic representation of the pole distribution for the transfer matrix $H_b(s)$ in the complex s -plane.

Proposition 2.1 (Pole Structure and Minnaert Resonance). *Under Assumption 2, and assuming that the physical input operator $B^{\text{in}}(s)$ is analytic in \mathbb{C} , the microscopic transfer matrix $H_b(s)$ defined in (2.14) satisfies the following properties:*

(i) *(Meromorphic structure of the transfer matrix)*

The transfer matrix $H_b(s)$ admits a meromorphic continuation to \mathbb{C} . In particular, it is meromorphic in the half-plane

$$\mathcal{S}_{-\sigma_0} := \left\{ s \in \mathbb{C} : \text{Re}(s) > -\sigma_0 \right\},$$

and its poles are contained in $\left\{ s : \det(\mathcal{D}(s) + s^2 \mathcal{Q}(s, \varepsilon)) = 0 \right\}$.

(ii) *(Discrete Poles and Asymptotic Cluster Separation)*

Let \mathcal{P} denote the discrete set of poles of H_b within $\mathcal{S}_{-\sigma_0}$. Due to the macroscopic material detuning, the dominant principal mode of each cluster $\alpha \in \{1, 2, \dots, N\}$ corresponds to a distinguished simple pole near its local unperturbed frequency $i\omega_{M,\alpha}$:

$$s_{\alpha,1}^* = -\eta_{\alpha,1} + i\omega_{\alpha,1}(\varepsilon), \quad \eta_{\alpha,1}, \omega_{\alpha,1}(\varepsilon) > 0.$$

Moreover, there exists $\varepsilon_0 > 0$ and a constant $g_0 > 0$ such that for all $\varepsilon \in (0, \varepsilon_0]$, the pole $s_{\alpha,1}^*$ is rigorously isolated from the complementary spectrum by an asymptotically scaled gap:

$$\text{dist}(s_{\alpha,1}^*, \mathcal{P} \setminus \{s_{\alpha,1}^*\}) \geq g_0 \varepsilon^{1-p} > 0.$$

In addition to that the generic disjointness ($\omega_{M,\alpha} \neq \omega_{M,\beta}$), guarantees distinct cluster principle dominant poles are strictly isolated by an $\mathcal{O}(1)$ spectral distance, quantified as:

$$|s_{M,\alpha}^*(\varepsilon) - s_{M,\beta}^*(\varepsilon)| = |\omega_{M,\alpha} - \omega_{M,\beta}| + \mathcal{O}(\varepsilon^{1-p}) \geq \Delta_\omega > 0, \quad (2.15)$$

where $\Delta_\omega := \frac{1}{2} \min_{\omega_{M,\beta} \neq \omega_{M,\alpha}} |\omega_{M,\alpha} - \omega_{M,\beta}|$.

(iii) (Residue Expansion at the Distinguished Pole)

Assuming the m -th resonant mode of cluster α is not annihilated by the input/output projections, $H_b(s)$ admits a strict Laurent expansion in the neighborhood U of $s_{\alpha,m}^*$:

$$H_b(s) = \frac{R_{\alpha,m}}{s - s_{\alpha,m}^*} + H_{\text{reg}}(s),$$

where the residue $R_{\alpha,m} \in \mathbb{C}^{M \times M} \setminus \{\mathbf{0}\}$ and $H_{\text{reg}}(s)$ is bounded and analytic in U .

Proof. See Section 5 for the details.

Assumption 3 (Cluster-level transducer accessibility). Let $\mathcal{K}_{\text{tr}} \Subset (0, \infty)$ be a compact frequency set containing the operational Minnaert bands

$$I_M = \bigcup_{\alpha=1}^N I_\alpha(\varepsilon)$$

introduced below. For transducer locations x_m^{tr} ($1 \leq m \leq M_{\text{tr}}$) and macroscopic cluster centers y_α ($1 \leq \alpha \leq N$), define the cluster-level trace matrix $\tilde{G}_{\text{tr}}(s) \in \mathbb{C}^{N \times M_{\text{tr}}}$ via

$$\tilde{G}_{\text{tr}}(s) := (G_s(y_\alpha, x_m^{\text{tr}}))_{1 \leq \alpha \leq N, 1 \leq m \leq M_{\text{tr}}}, \quad (2.16)$$

We assume $M_{\text{tr}} \geq N$ and the transducer geometry satisfies the uniform lower bound

$$\inf_{\omega \in \mathcal{K}_{\text{tr}}} \sigma_{\min}(\tilde{G}_{\text{tr}}(i\omega)) \geq c_{\text{tr}} > 0. \quad (2.17)$$

The geometric condition (2.17) holds for sufficiently distant transducers $x_m^{\text{tr}} = R_m \theta_m$ ($R_m \gg 1$, $\theta_m \in \mathbb{S}^2$). Indeed, the far-field expansion

$$G_{i\omega}(y_\alpha, x_m^{\text{tr}}) = c_m(\omega) e^{i(\omega/c_0)\theta_m \cdot y_\alpha} + \mathcal{O}(R_m^{-1}),$$

with $c_m(\omega) \neq 0$, shows that \tilde{G}_{tr} asymptotically acts as a multi-static sampling far-field response matrix for point sources at the cluster centers (well known in MUSIC-type algorithms). The underlying patterns $\{e^{i(\omega/c_0)\theta \cdot y_\alpha}\}_{\alpha=1}^N$ are linearly independent on \mathbb{S}^2 ; otherwise, Rellich's lemma and unique continuation would force the associated radiating field to vanish identically outside the cluster centers, contradicting the point singularities at y_α . Consequently, a choice of $M_{\text{tr}} \geq N$ distinct directions ensures $\text{rank}(\tilde{G}_{\text{tr}}) = N$, a property that persists uniformly on \mathcal{K}_{tr} for large finite R_m .

The microscopic trace matrix $G_{\text{tr}}(s) := (G_s(z_i, x_m^{\text{tr}})) \in \mathbb{C}^{M \times M_{\text{tr}}}$ satisfies

$$G_s(z_i, x_m^{\text{tr}}) = G_s(y_\alpha, x_m^{\text{tr}}) + \mathcal{O}(r_\varepsilon), \quad r_\varepsilon := \max_{\alpha} \max_{i \in \mathcal{I}_\alpha} |z_i - y_\alpha|, \quad (2.18)$$

for all $i \in \mathcal{G}_\alpha$ and $s \in i\mathcal{K}_{\text{tr}}$. Let $V_{\text{dom}}^\varepsilon, W_{\text{dom}}^\varepsilon \in \mathbb{C}^{M \times N}$ denote the biorthogonal principal cluster modes, satisfying $(W_{\text{dom}}^\varepsilon)^* V_{\text{dom}}^\varepsilon = I_N$. By the pole expansion of $H_b(s)$, the principal part of $\mathcal{H}_{\text{ext}}^\varepsilon(s)$ on I_M evaluates to

$$H_{\text{dom}}^\varepsilon(s) := B_{\text{out}} V_{\text{dom}}^\varepsilon \text{diag} \left(\frac{r_\alpha^\varepsilon}{s - s_{M,\alpha}^*} \right)_{\alpha=1}^N (W_{\text{dom}}^\varepsilon)^* G_{\text{tr}}(s). \quad (2.19)$$

Provided these modes are non-annihilated by the input-output projections, the macroscopic rank condition (2.17) and the $\mathcal{O}(r_\varepsilon)$ trace perturbation ensure a uniform spectral bound. Specifically, for sufficiently small ε and all $\omega \in I_M$, there exists $c_{\text{ext}} > 0$ such that

$$\sigma_{\min}(\mathcal{H}_{\text{ext}}^\varepsilon(i\omega)) \geq c_{\text{ext}} \frac{\varepsilon}{\eta_{\max}} \geq c > 0, \quad (2.20)$$

where $\eta_{\max} = \mathcal{O}(\varepsilon)$ is the maximal radiation damping scale. This guarantees a uniformly bounded right inverse for the physical control operator on the operational bands.

2.4 Spectral Isolation and Generic Controllability

Let $\Lambda := \{\hat{\omega}_\ell\}_{\ell=1}^L$ denote distinct Dirichlet angular eigenfrequencies, with eigenspaces $H_\ell := \text{span}\{\phi_\ell^{(j)}\}_{j=1}^{m_\ell}$. Then, the global target subspace H_M and its total dimension N_M are constructed as follows:

$$H_M := \bigoplus_{\ell=1}^L H_\ell, \quad N_M := \sum_{\ell=1}^L m_\ell.$$

Following Assumption 2, we take $N \geq N_M$ macroscopic clusters centered at $\mathbf{y} = (y_1, \dots, y_N) \in \Omega^N$. Let $\tau : \{1, \dots, N\} \rightarrow \{1, \dots, L\}$ be a surjective map. The parameters of cluster α are tuned such that its principal perturbed Minnaert pole satisfies $\text{Im}(s_{M,\alpha}^*(\varepsilon)) = \hat{\omega}_{\tau(\alpha)}$.

Proposition 2.2 (Spectral Isolation). *Let $I_\alpha(\varepsilon) := [\hat{\omega}_{\tau(\alpha)} - \delta(\varepsilon), \hat{\omega}_{\tau(\alpha)} + \delta(\varepsilon)]$ with $\delta(\varepsilon) \in (0, \frac{g_0}{2}\varepsilon^{1-p})$. Then, we have*

$$\text{dist}(I_\alpha(\varepsilon), \{\omega_k\}_{k \geq 1} \setminus \{\hat{\omega}_{\tau(\alpha)}\}) \geq \frac{\Delta_\omega}{2} > 0, \quad \forall \alpha \in \{1, \dots, N\}, \quad (2.21)$$

where $\Delta_\omega > 0$ is the uniform macroscopic spectral gap.

Proof. The proposition follows trivially from Step 6 of Proposition 2.1(ii) and the strict separation of the Dirichlet eigenvalues. \blacksquare

We define the composite Minnaert resonant band as the union of these isolated local bands ($I_\alpha \cap I_\beta = \emptyset$ for $\alpha \neq \beta$):

$$I_M := \bigcup_{\alpha=1}^N I_\alpha(\varepsilon). \quad (2.22)$$

Given an orthonormal basis $\Psi := (\psi_1, \dots, \psi_{N_M})^\top$ of H_M , define the spatial coupling matrix $C_M(\mathbf{y}) \in \mathbb{R}^{N_M \times N}$ by $[C_M(\mathbf{y})]_{i\alpha} := \psi_i(y_\alpha)$.

Proposition 2.3 (Generic Rank Condition). *For $N \geq N_M$, $\text{rank}(C_M(\mathbf{y})) = N_M$ for Lebesgue almost every macroscopic cluster configuration $\mathbf{y} \in \Omega^N$.*

Proof. We begin by defining $F : \Omega^{N_M} \rightarrow \mathbb{R}$ by $F(y_1, \dots, y_{N_M}) := \det(\psi_i(y_j))_{i,j=1}^{N_M}$. The real-analyticity of Dirichlet eigenfunctions in Ω implies F is real-analytic. Because $\{\psi_i\}_{i=1}^{N_M}$ are linearly independent in $L^2(\Omega)$, $F \not\equiv 0$. Therefore, the zero set $\mathcal{Z}_{N_M} := F^{-1}(0)$ constitutes an analytic variety of Lebesgue measure zero, [12, Ch. 6, Th. 6.3.3]. For any $\mathbf{y} \in (\Omega^{N_M} \setminus \mathcal{Z}_{N_M}) \times \Omega^{N-N_M}$, the leading $N_M \times N_M$ principal submatrix of $C_M(\mathbf{y})$ is invertible.

Proposition 2.3 formally embeds the localized problem into the classical framework of finite-dimensional exact controllability [22, Ch. 1]. The Galerkin projection onto H_{I_M} reduces the second-order wave dynamics to a first-order LTI system

$$\dot{z}(t) = Az(t) + B(\mathbf{y})u(t) \quad (2.23)$$

on the state space \mathbb{R}^{2N_M} , where $z = (\mathbf{p}^\top, \dot{\mathbf{p}}^\top)^\top$. The system operator is the block matrix $A = \begin{pmatrix} 0 & I \\ -c_0^2 \Lambda & 0 \end{pmatrix}$ with spectrum $\sigma(A) = \{\pm ic_0 \omega_k\}_{k=1}^{N_M}$, and the input operator is $B(\mathbf{y}) = \begin{pmatrix} 0 \\ c_0^2 C_M(\mathbf{y}) \end{pmatrix}$. By the Hautus test [22, Sec. 1.5], exact controllability requires

$$\text{rank} \left[\lambda I_{2N_M} - A \mid B(\mathbf{y}) \right] = 2N_M \quad (2.24)$$

for all $\lambda \in \mathbb{C}$. Given the block structures of A and $B(\mathbf{y})$, this block-matrix rank condition is algebraically equivalent to the requirement that

$$\text{rank}(C_M(\mathbf{y})) = N_M.$$

The real-analyticity of the Dirichlet eigenfunctions ensures that the rank-deficient configurations form a proper analytic variety \mathcal{Z}_{N_M} . Consequently, its Lebesgue measure is zero ($\mathcal{L}(\mathcal{Z}_{N_M}) = 0$), strictly guaranteeing that the Hautus rank condition is generically satisfied.

Let us also mention that for simple geometries for Ω , as cubes, one can give appropriate distributions of the macroscopic centers y_α so that the matrix C_M is full rank, see Appendix of [20].

Assumption 4 (Subspace Controllability). *Assume $\mathbf{y} \notin \mathcal{Z}_{N_M} \times \Omega^{N-N_M}$. Consequently, we have*

$$\text{rank}(C_M(\mathbf{y})) = N_M,$$

ensuring the existence of a uniformly bounded right inverse $L_M \in \mathbb{R}^{N \times N_M}$ satisfying $C_M(\mathbf{y})L_M = I_{N_M}$.

Definition 4 (Multi-band source space on a finite time interval). *Let*

$$I_M = \bigcup_{\alpha=1}^N I_\alpha(\varepsilon)$$

be the separated union of the operational Minnaert bands. Since the control problem is posed on the finite time interval $[0, T]$, we define the componentwise band space by restriction from the real line. Namely, $q = (q_1, \dots, q_N)$ belongs to V_{I_M} if, for every $\alpha = 1, 2, \dots, N$, there exists an extension $\tilde{q}_\alpha \in H^1(\mathbb{R})$ such that

$$\tilde{q}_\alpha|_{[0, T]} = q_\alpha, \quad \text{supp } \tilde{q}_\alpha \subset I_\alpha(\varepsilon).$$

We use the induced norm from $V = H^1(0, T; \mathbb{R}^N)$. Thus V_{I_M} should be read as a finite-time, multi-channel restriction of globally band-limited source profiles.

Proposition 2.4 (Approximate Surjectivity on the Minnaert Band). *Let $V_{I_M} \subset V$ be the multi-channel band space of Definition 4. The α -th effective cluster-source component has temporal content in the band attached to the α -th cluster. Because the bands are separated, V_{I_M} is the direct product of the componentwise band-pass spaces corresponding to $I_\alpha(\varepsilon)$. For any fixed $T > 0$, there exist constants $\varepsilon_0, \beta, C_T > 0$ and a family of bounded linear operators $R_{I_M}^\varepsilon \in \mathcal{L}(V_{I_M}, U_{\text{tr}})$ for $\varepsilon \in (0, \varepsilon_0)$ satisfying:*

$$\sup_{\varepsilon \in (0, \varepsilon_0)} \|R_{I_M}^\varepsilon\|_{\mathcal{L}(V_{I_M}, U_{\text{tr}})} < \infty, \quad (2.25)$$

$$\|\mathcal{F}^\varepsilon R_{I_M}^\varepsilon q - q\|_V \leq C_T \varepsilon^\beta \|q\|_V, \quad \forall q \in V_{I_M}. \quad (2.26)$$

Proof. See Section 6.3 for the details.

2.5 Quantitative Estimation of the Intra-Cluster Spectral Gap

While Proposition 2.1(ii) establishes the qualitative separation of the dominant pole (the Perron–Frobenius eigenvalue) from the sub-radiant modes within a given cluster, this section provides a rigorous quantitative characterization of their precise spectral configuration.

Let cluster α consist of M_α bubbles with a spatial scaling $d_{ij} = \tilde{d}_{ij}\varepsilon^p$ for $p \in (0, 1)$. Evaluating the interaction kernel at the unperturbed Minnaert resonance $s = i\omega_{M,\alpha}$ yields the leading-order operator:

$$\tilde{C}_\alpha^{(0)} := \lim_{\varepsilon \rightarrow 0} \varepsilon^{p-1} \mathcal{Q}(i\omega_{M,\alpha}, \varepsilon) = \frac{C_\alpha}{4\pi} \mathcal{M}_\alpha, \quad (2.27)$$

where \mathcal{M}_α is the dimensionless interaction matrix with entries:

$$[\mathcal{M}_\alpha]_{ij} = (1 - \delta_{ij}) \tilde{d}_{ij}^{-1}. \quad (2.28)$$

By Kato’s analytic perturbation theory [11], the principal resonance shift is dictated by the spectral radius $\mu_1(\alpha) = \max \sigma(\mathcal{M}_\alpha)$, which is a simple eigenvalue by the Perron–Frobenius theorem [10, Ch. 8]. Driven by the qualitative properties established in Proposition 2.1(ii), these principal frequencies $\omega_{\alpha,1}$ are well-separated by design to closely approximate the target Dirichlet eigenvalues, yielding the asymptotic expansion:

$$\omega_{\alpha,1}(\varepsilon) = \omega_{M,\alpha} - \frac{\omega_{M,\alpha}^3 C_\alpha}{8\pi} \mu_1(\alpha) \varepsilon^{1-p} + \mathcal{O}(\varepsilon^{\min(1, 2-2p)}). \quad (2.29)$$

Since $\text{Tr}(\mathcal{M}_\alpha) = 0$, isolating the principal pole $s_{\alpha,1}^*$ requires a strictly positive spectral gap $\Delta\mu_\alpha := \mu_1(\alpha) - \mu_2(\alpha) > 0$. This defines the physical intra-cluster gap:

$$\Delta_{\text{gap}}^{(\alpha)}(\varepsilon) := \frac{\omega_{M,\alpha}^3 C_\alpha}{8\pi} \Delta\mu_\alpha \varepsilon^{1-p}. \quad (2.30)$$

We explicitly quantify $\Delta\mu_\alpha$ for two physical arrangements:

- (i) *Equidistant Cluster*: For uniform dimensionless distances $\tilde{d}_{ij} = 1$ (physically limited to $M_\alpha \leq 4$ for embeddings in \mathbb{R}^3 , representing a regular tetrahedron), the interaction matrix simplifies to $\mathcal{M}_\alpha = \mathbf{J} - \mathbf{I}$. The spectrum is $\sigma(\mathcal{M}_\alpha) = \{M_\alpha - 1, -1, \dots, -1\}$, yielding a discrete gap $\Delta\mu_\alpha = M_\alpha > 0$.
- (ii) *1D Uniform Lattice*: For a linear chain with spacing h_α , the distance is $\tilde{d}_{ij} = h_\alpha |i - j|$. This reduces \mathcal{M}_α to a scaled symmetric Toeplitz matrix $h_\alpha^{-1} \mathcal{J}^{(\alpha)}$ with entries:

$$[\mathcal{J}^{(\alpha)}]_{ij} = (1 - \delta_{ij}) |i - j|^{-1}. \quad (2.31)$$

By standard row-sum bounds for non-negative matrices [10], the spectral radius $\mu_1(\mathcal{J}^{(\alpha)})$ satisfies:

$$H_{M_\alpha-1} \leq \mu_1(\mathcal{J}^{(\alpha)}) \leq 2H_{\lfloor M_\alpha/2 \rfloor}, \quad H_n := \sum_{k=1}^n k^{-1}. \quad (2.32)$$

Furthermore, because the matrix $\mathcal{J}^{(\alpha)}$ is entrywise non-negative and irreducible (having strictly positive off-diagonal entries), the Perron–Frobenius theorem [10, Ch. 8] ensures that its largest eigenvalue is unique and strictly separated from the second eigenvalue, guaranteeing a positive spectral gap:

$$C_\alpha := \mu_1(\mathcal{J}^{(\alpha)}) - \mu_2(\mathcal{J}^{(\alpha)}) > 0. \quad (2.33)$$

Imposing the bandwidth restriction $\delta(\varepsilon) \in \left(0, \frac{1}{2} \min_\alpha \Delta_{\text{gap}}^{(\alpha)}(\varepsilon)\right)$ therefore rigorously isolates the principal pole $s_{\alpha,1}^*$ from all sub-radiant modes.

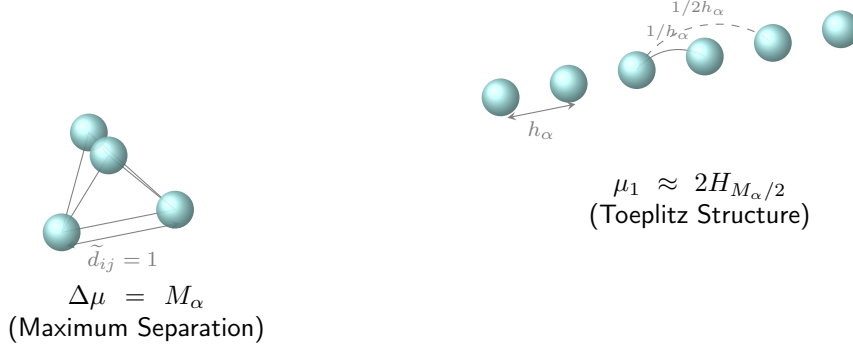


Figure 2: Cluster topologies: (Left) physical equidistant cluster and (Right) 1D uniform lattice with Toeplitz interaction structure.

2.6 Control Objective and Main Results

Problem. (Finite-dimensional tracking and efficient Minnaert realization) Given a final time $T > 0$, the target Dirichlet subspace H_M associated with the composite Minnaert band I_M , and a prescribed reference trajectory $p_r^{I_M} \in C^3([0, T]; H_M)$:

- (i) First construct the ideal cluster-source profile which gives exact tracking in the finite-dimensional Dirichlet spectral model.
- (ii) The physical question is then to realize this ideal profile by incident waves generated outside Ω .

The main result below concerns the efficient case where the ideal profile is realized through the separated Minnaert channels, with a uniform control cost. More precisely, find a family of admissible controls $\{\lambda^\varepsilon\}_{\varepsilon>0} \subset U_{\text{tr}}$ such that the generated physical pressure fields p^ε satisfy the uniform tracking condition:

$$\sup_{t \in [0, T]} \left(\|P_{I_M} p^\varepsilon(\cdot, t) - p_r^{I_M}(\cdot, t)\|_{H^1(\Omega)} + \|P_{I_M} \partial_t p^\varepsilon(\cdot, t) - \partial_t p_r^{I_M}(\cdot, t)\|_{L^2(\Omega)} \right) = \mathcal{O}(\varepsilon^\gamma)$$

for some constant $\gamma > 0$, subject to the uniform control cost bound:

$$\sup_{\varepsilon>0} \|\lambda^\varepsilon\|_{U_{\text{tr}}} < \infty.$$

The following theorem should be read in this sense. The abstract finite-dimensional tracking step is valid for arbitrary sufficiently smooth trajectories in H_M . The additional spectral localization to I_M enters only at the physical realization step: it is the condition under which the incident fields can generate the required ideal sources with uniformly bounded amplitudes. It is worth mentioning that the procedure suggested in this work is reconstructive.

Theorem 2.5 (Minnaert-Resonant Subspace Tracking). *Let $T > 0$. Define the physical control input space $U_{\text{tr}} := \{\lambda \in H^2(0, T; \mathbb{R}^{M_{\text{tr}}}) : \lambda(0) = \dot{\lambda}(0) = \mathbf{0}\}$ and the effective cluster-source space $V := H^1(0, T; \mathbb{R}^N)$. Let $I_M := \bigcup_{\alpha=1}^N I_\alpha(\varepsilon)$ be the composite Minnaert band, $V_{I_M} \subset V$ be the multi-band source space, and $H_M = \text{span}\{\psi_k\}_{k=1}^{N_M} \subset L^2(\Omega)$ be the N_M -dimensional target Dirichlet subspace ($N \geq N_M$) with orthogonal projection $P_{I_M} : L^2(\Omega) \rightarrow H_M$.*

Assume the foundational Material Parameter Scaling (Assump. 1), Topological Separation (Assump. 2), and Transducer Accessibility (Assump. 3) hold. Under these assumptions, the following properties are established in the Minnaert-resonant regime:

- (i) *Asymptotic Field Decomposition: The physical scattered field satisfies the decomposition $p^\varepsilon = p^{\text{eff}, \varepsilon} + \text{err}_\varepsilon$ on $\Omega \setminus \bar{D}$, where the projected remainder obeys the uniform estimate:*

$$\sup_{t \in [0, T]} \left(\|P_{I_M} \text{err}_\varepsilon(\cdot, t)\|_{H^1(\Omega \setminus \bar{D})} + \|P_{I_M} \partial_t \text{err}_\varepsilon(\cdot, t)\|_{L^2(\Omega \setminus \bar{D})} \right) \leq C_T \varepsilon^\mu, \quad (2.34)$$

with $p^{\text{eff}, \varepsilon}$ be the effective pressure generated by the realized cluster-level source vector $q^\varepsilon = \mathcal{F}^\varepsilon \lambda^\varepsilon$.

(ii) *Rank Condition:* The macroscopic cluster configuration $\mathbf{y} \in \Omega^N$ is generic (Prop. 2.3), strictly satisfying $\text{rank}(C_M(\mathbf{y})) = N_M$.

(iii) *Frequency-Domain Solvability and Surjectivity:* By the Pole Structure (Prop. 2.1), the exterior-to-cluster transfer matrix $\mathcal{H}_{\text{ext}}^\varepsilon(i\omega)$ has full row rank N for all $\omega \in I_M$ with radiation damping $\eta_{\text{max}} \sim \varepsilon$. Its pseudo-inverse satisfies the uniform frequency-domain bound (Prop. 6.6):

$$\sup_{\omega \in I_M} \|(\mathcal{H}_{\text{ext}}^\varepsilon(i\omega))^\dagger\|_2 \leq C \frac{\eta_{\text{max}}}{\varepsilon} \leq \kappa_0 < \infty, \quad (2.35)$$

ensuring that the physical actuator map $\mathcal{F}^\varepsilon : U_{\text{tr}} \rightarrow V$ admits a right inverse $R_{I_M}^\varepsilon$ satisfying the uniform time-domain cost estimate:

$$\|R_{I_M}^\varepsilon\|_{\mathcal{L}(V_{I_M}, U_{\text{tr}})} \leq \kappa_M. \quad (2.36)$$

Consequently, let $\mathbf{q}^{\text{ideal}} \in V_{I_M}$ be an ideal source profile generating the reference trajectory $p_r^{I_M} \in C^3([0, T]; H_M)$ via the ideal Dirichlet spectral wave equation:

$$\left(\frac{1}{c_0^2} \partial_{tt} - \Delta_D\right) p_r^{I_M}(x, t) = P_{I_M} \sum_{\alpha=1}^N q_\alpha^{\text{ideal}}(t) \delta_{y_\alpha}(x), \quad (x, t) \in \Omega \times (0, T], \quad (2.37)$$

subject to compatible rest initial conditions

$$p^{\text{eff}, \varepsilon}(\cdot, 0) = \partial_t p^{\text{eff}, \varepsilon}(\cdot, 0) = 0 \text{ and } p_r^{I_M}(\cdot, 0) = \partial_t p_r^{I_M}(\cdot, 0) = 0.$$

Then, there exist constants $\varepsilon_0, \gamma, C_T > 0$ independent of ε such that for all $\varepsilon \in (0, \varepsilon_0)$, the explicit physical control vector $\boldsymbol{\lambda}^\varepsilon := R_{I_M}^\varepsilon \mathbf{q}^{\text{ideal}} \in U_{\text{tr}}$ yields a realized physical scattered pressure field p^ε satisfying the uniform tracking bound:

$$\sup_{t \in [0, T]} \left(\|P_{I_M}(p^\varepsilon - p_r^{I_M})(\cdot, t)\|_{H^1(\Omega \setminus \bar{D})} + \|P_{I_M} \partial_t (p^\varepsilon - p_r^{I_M})(\cdot, t)\|_{L^2(\Omega \setminus \bar{D})} \right) \leq C_T \varepsilon^\gamma, \quad (2.38)$$

with an associated physical control cost bounded by

$$\|\boldsymbol{\lambda}^\varepsilon\|_{U_{\text{tr}}} \leq \kappa_M \|\mathbf{q}^{\text{ideal}}\|_V.$$

In (2.37), $P_{I_M} \delta_{y_\alpha}$ is defined by duality, namely $P_{I_M} \delta_{y_\alpha} := \sum_{k=1}^{N_M} \psi_k(y_\alpha) \psi_k$, so that $\langle P_{I_M} \delta_{y_\alpha}, \varphi \rangle = \varphi(y_\alpha)$, $\varphi \in H_M$. Hence (2.37) is an equation in H_M .

Remark 2.6. We strictly require the target source profile to reside in the multi-band space V_{I_M} to guarantee physical realizability at a bounded cost. While the ideal tracking construction holds for arbitrary trajectories, attempting to track temporal components outside the Minnaert resonance channels will result in a physical control cost that diverges as $\varepsilon \rightarrow 0$. The technical nuances of reconciling finite-time tracking with band-limited signal constraints are detailed in Section 6.

Remark 2.7 (Comparison with Thermo-Plasmonic Heat Tracking). While related to the thermo-plasmonic feedback framework in [20], the present setting differs mathematically in two fundamental ways. First, because the ideal PDE dynamics (2.2) are hyperbolic and conservative rather than parabolic, stabilization cannot rely on intrinsic semigroup decay; thus, tracking is strictly formulated on the finite spectral band H_J . Second, as used in [20], while plasmonic resonance merely improves the conditioning of the realization map, the Minnaert resonance rigorously dictates the gain and invertibility of $H_b(s)$, rendering it the central enabler for effective pressure tracking.

Tracking as an inverse problem for the control-to-state map. Once the dynamics are projected onto H_M , the actuation design problem becomes: find actuator signals (or, in the bubble realisation, the corresponding physical parameters) so that the modal coefficients of the solution match a prescribed reference \mathbf{p}_r (either at a terminal time T or over a time window). In operator form this amounts to solving a linear equation of the first kind on the finite-dimensional cluster-source space,

$$\mathcal{K}_M(\mathbf{q}) = \mathbf{p}_r,$$

where \mathcal{K}_M denotes the reduced control-to-state map induced by the projected wave propagator and the point-actuator coupling matrix $C_M = [\psi_k(y_\alpha)]$. Existence and robustness of tracking therefore **reduces to** the existence of a right-inverse of \mathcal{K}_M with controlled norm (equivalently, on uniform conditioning of its matrix representation). The Minnaert regime improves this conditioning through resonant amplification of the bubble monopole response, whereas away from resonance the same inverse problem becomes ill-conditioned under the physical actuation constraints.

Organisation of the paper

The remainder of this paper is organised as follows. Section 3 formulates the wave equation with ideal point actuators, proving exact tracking for C^3 trajectories via the coupling matrix inverse L_M . Section 4 derives the time-domain asymptotic expansions and localises the scattered field model to the bounded domain Ω . Section 5 provides a meromorphic analysis of the bubble transfer matrix $H_b(s)$ and characterises the isolated Minnaert poles. Section 6 demonstrates the approximate surjectivity of the bubble actuator map on the resonant band, overcoming the non-resonant divergence problem. Section 7 proves the main tracking result (Theorem 2.5) using energy-based error estimates as $\varepsilon \rightarrow 0$.

3 Ideal Point-Actuator Tracking

In this section we formulate the controlled wave equation on Ω with point actuators at the macroscopic cluster centers y_α , and prove an exact tracking result on a finite-dimensional spectral subspace.

3.1 Abstract formulation and well-posedness

We consider the point-actuated wave equation on a bounded domain $\Omega \subset \mathbb{R}^3$ with homogeneous Dirichlet boundary conditions.

$$\begin{cases} \frac{1}{c_0^2} \partial_t^2 p - \Delta p = \sum_{\alpha=1}^N q_\alpha(t) \delta_{y_\alpha} & \text{in } \Omega \times (0, T), \\ p = 0 & \text{on } \partial\Omega \times (0, T), \\ p(\cdot, 0) = 0, \quad \partial_t p(\cdot, 0) = 0. \end{cases} \quad (3.1)$$

In dimension three, the right-hand side does not belong to the dual of the standard energy space, so (3.1) cannot be interpreted directly as a well-posed evolution problem in $H_0^1(\Omega) \times L^2(\Omega)$. This problem can also be treated by transposition/duality in spaces associated with $D(-\Delta_D)'$, see [13, 16, 22]. Since we are interested here in a finite-dimensional tracking system, we therefore adopt a Galerkin (band-limited) formulation.

Let $\{\psi_k\}_{k \geq 1}$ be the Dirichlet Laplacian eigenfunctions, forming an orthonormal basis of $L^2(\Omega)$, and let $H_M := \text{span}\{\psi_1, \dots, \psi_{N_M}\}$ denote the N_M -dimensional target subspace corresponding to the macroscopic Minnaert composite band I_M , with orthogonal projection $P_{I_M} : L^2(\Omega) \rightarrow H_M$. Given the cluster-level source vector $\mathbf{q} = (q_1, \dots, q_N)^\top \in L^2(0, T; \mathbb{R}^N)$, we seek

$$p_M(t) \in H_M, \quad t \in [0, T],$$

such that, for a.e. $t \in (0, T)$,

$$\frac{1}{c_0^2} \langle \partial_t^2 p_M(\cdot, t), \varphi \rangle + \langle \nabla p_M(\cdot, t), \nabla \varphi \rangle = \sum_{\alpha=1}^N q_\alpha(t) \varphi(y_\alpha), \quad \forall \varphi \in H_M, \quad (3.2)$$

with trivial projected initial data

$$p_M(\cdot, 0) = 0, \quad \partial_t p_M(\cdot, 0) = 0. \quad (3.3)$$

Since H_M is finite-dimensional and spanned by smooth eigenfunctions, we have $H_M \subset H^2(\Omega)$, and in particular $\varphi(y_\alpha)$ is well-defined for all $\varphi \in H_M$. Hence the right-hand side of (3.2) is strictly well-defined.

Proposition 3.1 (Galerkin well-posedness from rest). *Let $T > 0$ and $\mathbf{q} \in L^2(0, T; \mathbb{R}^N)$. Then the Galerkin problem (3.2)–(3.3) admits a unique solution*

$$p_M \in H^2(0, T; H_M).$$

Writing $p_M(x, t) = \sum_{k=1}^{N_M} p_k(t) \psi_k(x)$, the coefficients satisfy the decoupled forced oscillator system

$$\ddot{p}_k(t) + \omega_k^2 p_k(t) = c_0^2 \sum_{\alpha=1}^N q_\alpha(t) \psi_k(y_\alpha), \quad k = 1, \dots, N_M, \quad (3.4)$$

with initial data $p_k(0) = 0$ and $\dot{p}_k(0) = 0$. Moreover, there exists a constant $C_{T,M} > 0$ (depending on T and the target subspace H_M , but not on \mathbf{q}) such that the energy satisfies the bound

$$\sup_{t \in [0, T]} \left(\|\nabla p_M(\cdot, t)\|_{L^2(\Omega)} + \|\partial_t p_M(\cdot, t)\|_{L^2(\Omega)} \right) \leq C_{T,M} \|\mathbf{q}\|_{L^2(0, T; \mathbb{R}^N)}. \quad (3.5)$$

Proof. Substituting the expansion $p_M(x, t) = \sum_{k=1}^{N_M} p_k(t) \psi_k(x)$ into the weak formulation (3.2) and choosing test functions $\varphi = \psi_k$, we obtain

$$\frac{1}{c_0^2} \ddot{p}_k(t) + \lambda_k p_k(t) = \sum_{\alpha=1}^N q_\alpha(t) \psi_k(y_\alpha).$$

Multiplying by c_0^2 and setting $\omega_k^2 = c_0^2 \lambda_k$ yields (3.4). Since $\psi_k \in C^\infty(\overline{\Omega})$, the quantities $\psi_k(y_\alpha)$ are well-defined.

Introducing the modal vector $\mathbf{p}^M(t) := (p_1(t), \dots, p_{N_M}(t))^\top$, the diagonal matrix $\Lambda_M := \text{diag}(\omega_1^2, \dots, \omega_{N_M}^2)$, and the geometric modal evaluation matrix $C_M(\mathbf{y}) \in \mathbb{R}^{N_M \times N}$ with $[C_M(\mathbf{y})]_{k\alpha} := \psi_k(y_\alpha)$, the system can be written compactly as

$$\ddot{\mathbf{p}}^M(t) + \Lambda_M \mathbf{p}^M(t) = c_0^2 C_M(\mathbf{y}) \mathbf{q}(t). \quad (3.6)$$

This is a linear second-order ODE in \mathbb{R}^{N_M} with L^2 forcing, and therefore admits a unique solution $\mathbf{p}^M \in H^2(0, T; \mathbb{R}^{N_M})$ subject to $\mathbf{p}^M(0) = 0$ and $\dot{\mathbf{p}}^M(0) = 0$. This implies $p_M \in H^2(0, T; H_M)$. We now derive the energy estimate. Define the modified modal energy

$$E_M(t) := \frac{1}{2} \left(|\Lambda_M^{1/2} \mathbf{p}^M(t)|^2 + |\dot{\mathbf{p}}^M(t)|^2 \right).$$

Differentiating and substituting the dynamics from (3.6), we obtain

$$E'_M(t) = \dot{\mathbf{p}}^M(t) \cdot (c_0^2 C_M(\mathbf{y}) \mathbf{q}(t)).$$

By the Cauchy–Schwarz inequality and the matrix operator norm,

$$E'_M(t) \leq c_0^2 |\dot{\mathbf{p}}^M(t)| \|C_M(\mathbf{y})\| |\mathbf{q}(t)| \leq c_0^2 \sqrt{2E_M(t)} \|C_M(\mathbf{y})\| |\mathbf{q}(t)|.$$

Setting $y(t) := \sqrt{E_M(t)}$ and noting $y(0) = 0$, we obtain $y'(t) \leq c_0^2 \|C_M(\mathbf{y})\| |\mathbf{q}(t)|$ for a.e. $t \in (0, T)$. Integrating over $[0, t]$ yields

$$\sup_{t \in [0, T]} y(t) \leq c_0^2 \|C_M(\mathbf{y})\| \sqrt{T} \|\mathbf{q}\|_{L^2(0, T; \mathbb{R}^N)}.$$

Finally, noting that $|\dot{\mathbf{p}}^M(t)| = \|\partial_t p_M(\cdot, t)\|_{L^2(\Omega)}$ and translating the stiffness term via $\omega_k^2 = c_0^2 \lambda_k$:

$$|\Lambda_M^{1/2} \mathbf{p}^M(t)|^2 = \sum_{k=1}^{N_M} c_0^2 \lambda_k |p_k(t)|^2 = c_0^2 \|\nabla p_M(\cdot, t)\|_{L^2(\Omega)}^2,$$

the bounds on $y(t)$ directly establish (3.5). ■

3.2 Tracking on a finite spectral subspace

Let $T > 0$ and $\mathbf{p}_r \in C^3([0, T]; \mathbb{R}^{N_M})$ be a target reference trajectory for the modes in the Minnaert band. Define the corresponding reference field

$$p_r^{I_M}(x, t) := \sum_{k=1}^{N_M} (\mathbf{p}_r(t))_k \psi_k(x).$$

Since the wave equation (3.1) starts from rest, we assume that the reference trajectory also starts from rest to ensure compatibility:

$$(\mathbf{p}_r(0))_k = 0, \quad (\dot{\mathbf{p}}_r(0))_k = 0, \quad k = 1, \dots, N_M. \quad (3.7)$$

By Proposition 2.3, the macroscopic coupling matrix $C_M(\mathbf{y}) \in \mathbb{R}^{N_M \times N}$ has full row rank N_M for $N \geq N_M$. Equivalently, there exists a right inverse $L_M \in \mathbb{R}^{N \times N_M}$ such that

$$C_M(\mathbf{y})L_M = I_{N_M}.$$

Theorem 3.2 (Exact tracking on the target subspace). *Let $N \geq N_M$ and satisfy the generic rank condition. Let $T > 0$ and $\mathbf{p}_r \in C^3([0, T]; \mathbb{R}^{N_M})$ satisfying (3.7). Define the ideal actuator control vector:*

$$\mathbf{q}^{\text{ideal}}(t) := \frac{1}{c_0^2} L_M (\ddot{\mathbf{p}}_r(t) + \Lambda_M \mathbf{p}_r(t)), \quad t \in [0, T]. \quad (3.8)$$

Let \mathbf{p}^M be the unique solution of (3.6) driven by $\mathbf{q} = \mathbf{q}^{\text{ideal}}$ with zero initial data. Then

$$\mathbf{p}^M(t) = \mathbf{p}_r(t), \quad \dot{\mathbf{p}}^M(t) = \dot{\mathbf{p}}_r(t), \quad t \in [0, T],$$

and consequently

$$P_{I_M} p(\cdot, t) = p_r^{I_M}(\cdot, t), \quad P_{I_M} \partial_t p(\cdot, t) = \partial_t p_r^{I_M}(\cdot, t), \quad t \in [0, T].$$

Proof. By Proposition 3.1, for any $\mathbf{q} \in L^2(0, T; \mathbb{R}^N)$ the system (3.6) admits a unique solution $\mathbf{p}^M \in H^2(0, T; \mathbb{R}^{N_M})$. In particular, the control (3.8) is admissible since $\mathbf{p}_r \in C^3([0, T]; \mathbb{R}^{N_M})$.

Using (3.8) and the identity $C_M(\mathbf{y})L_M = I_{N_M}$, we obtain

$$c_0^2 C_M(\mathbf{y}) \mathbf{q}^{\text{ideal}}(t) = C_M(\mathbf{y}) L_M (\ddot{\mathbf{p}}_r(t) + \Lambda_M \mathbf{p}_r(t)) = \ddot{\mathbf{p}}_r(t) + \Lambda_M \mathbf{p}_r(t).$$

Thus (3.6) becomes

$$\ddot{\mathbf{p}}^M(t) + \Lambda_M \mathbf{p}^M(t) = \ddot{\mathbf{p}}_r(t) + \Lambda_M \mathbf{p}_r(t), \quad t \in [0, T].$$

Define the tracking error $\mathbf{e}(t) := \mathbf{p}^M(t) - \mathbf{p}_r(t)$. Then \mathbf{e} satisfies

$$\ddot{\mathbf{e}}(t) + \Lambda_M \mathbf{e}(t) = 0, \quad t \in [0, T],$$

with initial conditions

$$\mathbf{e}(0) = 0, \quad \dot{\mathbf{e}}(0) = 0,$$

by (3.7). Since this is a homogeneous linear ODE with constant coefficients, uniqueness implies $\mathbf{e} \equiv 0$ on $[0, T]$, which yields the result. \blacksquare

Remark 3.3 (Why we do not pursue feedback stabilization of the truncated wave system).

The reduced model (3.6) is a finite-dimensional, lossless second-order system. Thus, in open loop, the homogeneous error dynamics $\ddot{\mathbf{e}} + \Lambda_M \mathbf{e} = 0$ conserve energy and do not exhibit decay. For each fixed N_M , one could in principle add a feedback term (e.g. pole placement) to render the closed-loop N_M -mode error exponentially stable. We do not follow this route here for two reasons.

(i) Lack of uniformity as N_M grows. *Even when a stabilizing gain exists for each fixed N_M , the corresponding decay rates and gain bounds typically deteriorate as $N_M \rightarrow \infty$ for wave dynamics with finitely many localized actuators. In particular, high-frequency modes become increasingly difficult to*

control/observe, and there is in general no exponential decay estimate that is uniform in N_M ; the required feedback gains may blow up as N_M increases.

(ii) Spillover for the full PDE. A controller designed on the truncated system acts on the physical (infinite-dimensional) wave equation and may excite unmodelled modes (the complement of H_M). In the absence of physical damping these components do not decay, so stabilization of the truncated model does not automatically translate into stabilization of the full lossless PDE.

Instead, our strategy is finite-horizon tracking on the chosen mode set, as in Theorem 3.2, combined with a physically realizable right-inversion step (Level 1) that produces the effective forcing coefficients from incident fields. In the bubbly setting, the Minnaert resonance improves the gain/conditioning of this realization map, and hence allows one to increase the number of tracked modes while keeping the actuation within feasible levels.

4 Bubble Dynamics and the Transfer Matrix

We now connect the ideal point-actuator model to the physical bubble model, in which the required effective sources are generated by external incident fields through a delayed, finite-dimensional multiple-scattering system.

4.1 Scattered field as a superposition of retarded monopoles

Recall the physical transmission problem (2.5) defined in Section 2.2. The incident field in the homogeneous medium generated by the M_{tr} external transducers at $x_m^{\text{tr}} \subset \mathbb{R}^3 \setminus \bar{\Omega}$ with signals $\lambda \in U_{\text{tr}}$ is given by the superposition:

$$u^{\text{in}}(x, t) = \sum_{m=1}^{M_{\text{tr}}} \frac{\rho_c}{4\pi|x - x_m^{\text{tr}}|} \lambda_m(t - c_0^{-1}|x - x_m^{\text{tr}}|). \quad (4.1)$$

We follow the setting of [18, 19]. Under the Assumptions 1 and 2, the scattered field $u^{\text{sc}} := u - u^{\text{in}}$ admits a rigorous multipole expansion.

Proposition 4.1 (Scattered field expansion and bubble system). *Under the Assumptions 1 and 2 on the bubble geometry and the high-contrast scaling, there exist:*

1. constants $C_i(\varepsilon) = \varepsilon \tilde{C}_i$, where $\tilde{C}_i > 0$ are constants independent of ε and depending only on the geometry and contrasts of the bubble D_i ;
2. scalar functions $Y_i \in C^2([0, T])$, $i = 1, \dots, M$, solving a finite-dimensional delayed system (see (4.5) below);
3. a remainder $R^\varepsilon \in C([0, T]; L_{\text{loc}}^2(\mathbb{R}^3 \setminus \bar{D}))$;

such that for x in bounded regions away from the cluster,

$$u^{\text{sc}}(x, t) = - \sum_{i=1}^M C_i(\varepsilon) \frac{1}{4\pi|x - z_i|} Y_i(t - c_0^{-1}|x - z_i|) + R^\varepsilon(x, t), \quad t \in [0, T], \quad (4.2)$$

and, for the chosen bounded localization domain Ω containing all bubbles, there exist $\mu > 0$ and $C_{T, \Omega} > 0$ independent of ε such that

$$\sup_{t \in [0, T]} \|R^\varepsilon(\cdot, t)\|_{L^2(\Omega \setminus \bar{D})} \leq C_{T, \Omega} \varepsilon^\mu. \quad (4.3)$$

Here, $(Y_i)_{i=1}^M$ is the vector solution to the following non-homogeneous second-order matrix differential equation with zero initial conditions:

$$\begin{cases} \omega_M^{-2} \frac{d^2}{dt^2} Y_i(t) + Y_i(t) + \sum_{\substack{j=1 \\ j \neq i}}^M q_{ij} \frac{d^2}{dt^2} Y_j(t - \tau_{ij}) = \frac{\partial^2}{\partial t^2} u^{\text{in}}(z_i, t), & \text{in } (0, T), \\ Y_i(0) = \frac{d}{dt} Y_i(0) = 0, \end{cases} \quad (4.4)$$

where $\omega_M^{-2} = \frac{\rho_c}{2\bar{\kappa}_{b,i}} \Lambda_{\partial B_i}$ represents the inverse square of the Minnaert frequency ω_M of the bubble D_i (see, for instance, [4, 8]). For each $i = 1, \dots, M$, the parameters satisfy

$$\omega_M^{-2} > 0, \quad \tau_{ij} = c_0^{-1}|z_i - z_j| \geq 0 \quad (j = 1, \dots, M), \quad q_{ij} = \frac{C_j(\varepsilon)}{4\pi|z_i - z_j|} \in \mathbb{R},$$

with the convention $q_{ii} = 0$ and $\tilde{C}_j := \text{vol}(B_j) \frac{\rho_c}{\bar{\kappa}_{b,j}}$. Also, $\Lambda_{\partial B_i} := \frac{1}{|\partial B_i|} \int_{\partial B_i} \int_{\partial B_i} \frac{(\mathbf{x} - \mathbf{y}) \cdot \nu_{\mathbf{x}}}{|\mathbf{x} - \mathbf{y}|} d\sigma_{\mathbf{x}} d\sigma_{\mathbf{y}}$ is a geometric constant. The well-posedness of the system of differential equations (4.4) is discussed in [18, Section 2.4]. In vector form, (4.4) can be written as

$$\mathcal{D} \ddot{\mathbf{Y}}(t) + \mathbf{Y}(t) + \mathcal{Q}[\ddot{\mathbf{Y}}](t) = \mathcal{F}(t), \quad \mathbf{Y}(0) = \dot{\mathbf{Y}}(0) = 0, \quad (4.5)$$

where (i) $\mathcal{D} := \text{diag}(d_1, \dots, d_M)$, (ii) $\mathcal{Q}[\ddot{\mathbf{Y}}](t)$ has components

$$(\mathcal{Q}[\ddot{\mathbf{Y}}](t))_i := \sum_{j \neq i} q_{ij} \ddot{Y}_j(t - \tau_{ij}), \quad \tau_{ij} := c_0^{-1}|z_i - z_j|,$$

and (iii) $\mathcal{F}(t) \in \mathbb{R}^M$ has i -th component $\frac{\partial^2}{\partial t^2} u^{in}(z_i, t)$.

Define

$$q_i^\varepsilon(t) := -C_i(\varepsilon) \tilde{Y}_i(t), \quad i = 1, \dots, M,$$

and $q^\varepsilon = (q_1^\varepsilon, \dots, q_M^\varepsilon)$. Then (4.2) becomes

$$u^{\text{sc}}(x, t) = \sum_{i=1}^M \frac{1}{4\pi|x - z_i|} q_i^\varepsilon(t - c_0^{-1}|x - z_i|) + R^\varepsilon(x, t). \quad (4.6)$$

Let us now introduce the retarded fundamental solution of the wave operator in the homogeneous medium:

$$\mathcal{G}_0(x, t; y) := \frac{\rho_c}{4\pi|x - y|} \delta(t - c_0^{-1}|x - y|), \quad x \neq y, \quad t > 0. \quad (4.7)$$

Given a time-dependent source $f \in \mathcal{S}'(\mathbb{R})$, the retarded field generated by a point source at $y \in \mathbb{R}^3$ is

$$\mathcal{W}[f; y](x, t) := (\mathcal{G}_0(\cdot - y, \cdot) *_t f)(x, t) = \frac{1}{4\pi|x - y|} f(t - c_0^{-1}|x - y|), \quad (4.8)$$

where f is extended by zero to negative times. Equivalently, using the representation (4.8), we introduce the effective scattered pressure

$$p^{\text{eff}, \varepsilon}(x, t) := \sum_{i=1}^M \mathcal{W}[q_i^\varepsilon; z_i](x, t).$$

For given T , we can find $\Omega, D \subset \Omega$, such that the physical scattered field is then compared to this effective field by

$$u^{\text{sc}}(x, t) = p^{\text{eff}, \varepsilon}(x, t) + \text{err}_\varepsilon(x, t), \quad (x, t) \in (\Omega \setminus \bar{D}) \times (0, T),$$

where the asymptotic estimate controls err_ε only away from the bubbles. Thus the following point-source equation is not asserted for the full physical field; it is the defining equation for the effective field:

$$\frac{1}{c_0^2} \partial_t^2 p^{\text{eff}, \varepsilon} - \Delta p^{\text{eff}, \varepsilon} = \sum_{i=1}^M q_i^\varepsilon(t) \delta_{z_i} \quad \text{in } \mathcal{D}'(\mathbb{R}^3 \times (0, T)). \quad (4.9)$$

4.2 Cluster reduction and localization to the bounded domain Ω

Restricting the effective field to the bounded observation domain Ω , one may first write the localized version of the M -bubble effective model as

$$\frac{1}{c_0^2} \partial_t^2 p_M^{\text{eff},\varepsilon} - \Delta p_M^{\text{eff},\varepsilon} = \sum_{i=1}^M q_i^\varepsilon(t) \delta_{z_i} \quad \text{in } \Omega \times (0, T), \quad (4.10)$$

understood after projection onto finite-dimensional Dirichlet spectral subspaces.

We now pass from the microscopic retarded representation to the cluster-output representation used by the control model. This is a reduction of the field representation, after the M -dimensional microscopic bubble system has determined the amplitudes q_i^ε . Let

$$r_\varepsilon := \max_{1 \leq \alpha \leq N} \max_{i \in \mathcal{I}_\alpha} |z_i - y_\alpha|$$

be the maximal cluster diameter. On observation sets separated from the bubbles, the retarded kernel $\mathcal{G}_0(x, t; z)$ is smooth in the source variable z for z near each cluster. Hence, for $i \in \mathcal{I}_\alpha$,

$$\mathcal{W}[q_i^\varepsilon; z_i] = \mathcal{W}[q_i^\varepsilon; y_\alpha] + \mathcal{O}(r_\varepsilon),$$

with the error measured in the same away-from-the-bubbles norms as in (4.2), provided the amplitudes are controlled in the corresponding time norms. Summing inside each cluster yields

$$p_M^{\text{eff},\varepsilon}(x, t) = \sum_{\alpha=1}^N \mathcal{W}[Q_\alpha^\varepsilon; y_\alpha](x, t) + \mathcal{R}_{\text{cl}}^\varepsilon(x, t), \quad Q_\alpha^\varepsilon(t) := (B_{\text{out}} \mathbf{q}_{\text{mic}}^\varepsilon(t))_\alpha = \sum_{i \in \mathcal{I}_\alpha} q_i^\varepsilon(t). \quad (4.11)$$

In the principal coherent Minnaert mode of cluster α , one may write

$$q_i^\varepsilon(t) = \tilde{q}_\alpha^\varepsilon(t) + \rho_i^\varepsilon(t), \quad i \in \mathcal{I}_\alpha,$$

where ρ_i^ε denotes the non-dominant intra-cluster component. Consequently

$$Q_\alpha^\varepsilon(t) = M_\alpha \tilde{q}_\alpha^\varepsilon(t) + \sum_{i \in \mathcal{I}_\alpha} \rho_i^\varepsilon(t).$$

Thus, on the selected principal cluster band, the effective cluster strength is $Q_\alpha^\varepsilon \simeq M_\alpha \tilde{q}_\alpha^\varepsilon$, while $\mathcal{R}_{\text{cl}}^\varepsilon$ and the non-dominant components are included in the final physical remainder.

Thus the localized actuator model used in the finite-dimensional tracking argument is the cluster-level effective model

$$\frac{1}{c_0^2} \partial_t^2 p_{\text{cl}}^{\text{eff},\varepsilon} - \Delta p_{\text{cl}}^{\text{eff},\varepsilon} = \sum_{\alpha=1}^N Q_\alpha^\varepsilon(t) \delta_{y_\alpha} \quad \text{in } \Omega \times (0, T). \quad (4.12)$$

In the rest of the paper, we write q_α^ε for this cluster-level coefficient Q_α^ε when no confusion is possible. Thus the symbol q_α in the ideal Dirichlet spectral model denotes the strength multiplying δ_{y_α} , not a single microscopic bubble amplitude. The physical field is then related to the effective one by

$$p^\varepsilon = p^{\text{eff},\varepsilon} + \text{err}_\varepsilon \quad \text{on } (\Omega \setminus \bar{D}) \times (0, T), \quad (4.13)$$

and the only error estimate used in the control argument is the projected bound

$$\sup_{t \in [0, T]} \left(\|P_{I_M} \text{err}_\varepsilon(\cdot, t)\|_{H^1(\Omega \setminus \bar{D})} + \|P_{I_M} \partial_t \text{err}_\varepsilon(\cdot, t)\|_{L^2(\Omega \setminus \bar{D})} \right) \leq C_T \varepsilon^\mu. \quad (4.14)$$

This is the form compatible with the asymptotic result of the bubbly transmission problem: the control is designed for $p^{\text{eff},\varepsilon}$, and the physical pressure p^ε is recovered up to err_ε .

Remark 4.2 (Dependence of the remainder on the excitation). *The bubbly transmission problem and the effective source amplitudes are linear in the incident excitation. In the estimates of [18, 19], the constants in projected remainder bounds such as (4.14) depend (at most) linearly on suitable norms of the incident field on $[0, T]$. Accordingly, when designing controls it is important to keep $\|\lambda^\varepsilon\|_{U_{\text{tr}}}$ uniformly bounded (or at least polynomially bounded) with respect to ε , so that the asymptotic error remains of order $\mathcal{O}(\varepsilon^\mu)$ on $[0, T]$. This loop is closed in the Minnaert regime once a uniformly bounded (or quantified) right inverse is available for the actuator map.*

We shall work on Ω with the effective field $p^{\text{eff},\varepsilon}$ satisfying (4.10); the physical field is denoted by p^ε and is compared to $p^{\text{eff},\varepsilon}$ through (4.13)–(4.14).

4.3 Laplace-domain transfer function of the bubble subsystem

To control the effective sources $q^\varepsilon(t) \in V$, we must invert the dynamical relationship between the external transducers and the bubble oscillations. We perform this analysis in the frequency domain. The effective sources at the bubble centers are defined by

$$q_i^\varepsilon(t) := -C_i(\varepsilon) Y_i(t), \quad q^\varepsilon(t) := (q_1^\varepsilon(t), \dots, q_M^\varepsilon(t))^\top = \mathcal{A}_b \mathbf{Y}(t),$$

where $\mathcal{A}_b := -\text{diag}(C_i(\varepsilon))_{i=1}^M$ is a diagonal matrix collecting the scaling coefficients.

The incident field is generated by M_{tr} transducers with signals $\lambda_m(t)$, $m = 1, \dots, M_{\text{tr}}$. Evaluated at the bubble centers, this defines an input vector $u^{\text{in}}(t) \in \mathbb{R}^{M_{\text{tr}}}$, which depends linearly on the signals $\lambda = (\lambda_1, \dots, \lambda_{M_{\text{tr}}})$.

Applying the Fourier–Laplace transform to the amplitude system, and using the zero initial conditions together with the translation identity

$$\mathcal{L}[\ddot{Y}_j(t - \tau_{ij})](s) = e^{-s\tau_{ij}} s^2 \widehat{Y}_j(s),$$

yields the matrix equation

$$(I + \mathcal{F}(s)) \widehat{\mathbf{Y}}(s) = \mathcal{V}(s), \quad \text{Re } s > \sigma_0,$$

where we define the diagonal unperturbed operator and the interaction matrix as

$$\mathcal{D}(s) = \text{diag}(\omega_M^{-2} s^2 + 1)_{i=1}^M, \quad \mathcal{Q}(s) = (q_{ij} e^{-s\tau_{ij}})_{i,j=1}^M,$$

and we set

$$\mathcal{F}(s) := \mathcal{D}(s)^{-1} s^2 \mathcal{Q}(s), \quad \mathcal{V}(s) := \mathcal{D}(s)^{-1} s^2 \widehat{\mathcal{F}}(s).$$

Here, $\widehat{\mathcal{F}}(s) = \mathcal{L}[\mathcal{F}(t)]$ represents the Laplace transform of the causal forcing vector, related to the incident field evaluated at the bubble centers. The function $\mathcal{V}(s)$ is analytic for $\text{Re } s > \sigma_0$. The physical parameters satisfy

$$\omega_M > 0, \quad \tau_{ij} = c_0^{-1} |z_i - z_j| \geq 0, \quad q_{ij} = \frac{C_j(\varepsilon)}{4\pi |z_i - z_j|} \in \mathbb{R},$$

with the convention $q_{ii} = 0$. By defining the dynamic interaction kernel

$$\mathcal{K}_{\text{dyn}}(s) := I + \mathcal{F}(s),$$

the Laplace system equation can be concisely written as

$$\mathcal{K}_{\text{dyn}}(s) \widehat{\mathbf{Y}}(s) = \mathcal{D}(s)^{-1} s^2 \widehat{\mathcal{F}}(s).$$

For $\text{Re } s > 0$ such that $\mathcal{K}_{\text{dyn}}(s)$ is invertible, we have

$$\widehat{\mathbf{Y}}(s) = \mathcal{K}_{\text{dyn}}(s)^{-1} \mathcal{D}(s)^{-1} s^2 \widehat{\mathcal{F}}(s).$$

Since the forcing $\mathcal{F}(t)$ depends linearly on the incident field $u^{\text{in}}(t)$, there exists a matrix-valued function $B^{\text{in}}(s)$ such that

$$\widehat{\mathcal{F}}(s) = B^{\text{in}}(s) \widehat{u}^{\text{in}}(s).$$

Defining the composite input matrix $B(s) := \mathcal{D}(s)^{-1}s^2B^{in}(s)$, we obtain

$$\widehat{Y}(s) = \mathcal{K}_{\text{dyn}}(s)^{-1}B(s)\widehat{u}^{in}(s).$$

Since $\widehat{q}^\varepsilon(s) = \mathcal{A}_b\widehat{Y}(s)$, it follows that

$$H_b(s) := \mathcal{A}_b\mathcal{K}_{\text{dyn}}(s)^{-1}B(s),$$

which explicitly provides the input-output map

$$\widehat{q}^\varepsilon(s) = H_b(s)\widehat{u}^{in}(s), \quad \text{Re } s > 0.$$

The poles of $H_b(s)$ represent the resonant frequencies of the coupled bubble system and are determined by the zeros of the characteristic determinant:

$$\mathcal{Z}(s) := \det(\mathcal{D}(s) + s^2\mathcal{Q}(s)) = 0. \quad (4.15)$$

In the unperturbed single-bubble case ($M = 1$, $\mathcal{Q}(s) = 0$), the interaction term vanishes and the condition for resonance simplifies to $\det \mathcal{D}(s) = 0$, or equivalently:

$$\omega_M^{-2}s^2 + 1 = 0. \quad (4.16)$$

This yields the purely imaginary roots $s = \pm i\omega_M$, which identify the fundamental Minnaert resonance. For systems comprising multiple bubbles ($M > 1$), the interaction matrix $\mathcal{Q}(s)$ perturbs these roots, resulting in a finite cluster of resonances distributed in the complex left half-plane.

5 Pole Structure and the Minnaert Resonance: Proof of Proposition 2.1

5.1 Proof of Proposition 2.1(1): Meromorphic structure of the transfer matrix

Proof. Substitution of $B(s)$ into $H_b(s)$ yields:

$$H_b(s, \varepsilon) = \mathcal{A}_b\mathcal{K}_{\text{dyn}}(s, \varepsilon)^{-1}\mathcal{D}(s)^{-1}s^2B^{in}(s).$$

Define the ε -dependent matrix pencil $P(s, \varepsilon) := \mathcal{D}(s)\mathcal{K}_{\text{dyn}}(s, \varepsilon) = \mathcal{D}(s) + s^2\mathcal{Q}(s, \varepsilon)$. Then the system becomes:

$$H_b(s, \varepsilon) = \mathcal{A}_bP(s, \varepsilon)^{-1}s^2B^{in}(s). \quad (5.1)$$

Since $\mathcal{D}(s)$ is a polynomial matrix and the entries $\mathcal{Q}_{ij}(s, \varepsilon) = q_{ij}(\varepsilon)e^{-s\tau_{ij}(\varepsilon)}$ are entire functions with respect to s , $P(s, \varepsilon)$ is an entire $M \times M$ matrix-valued function for any fixed $\varepsilon > 0$.

Let $f(s, \varepsilon) = \det P(s, \varepsilon)$. To establish that $f \neq 0$ with respect to s , consider the asymptotic behavior for $s = x \in \mathbb{R}^+$ as $x \rightarrow \infty$. Factoring the pencil:

$$P(x, \varepsilon) = \mathcal{D}(x) \left(I + \mathcal{D}(x)^{-1}x^2\mathcal{Q}(x, \varepsilon) \right).$$

Since $\mathcal{D}(x) = \text{diag}(\omega_{M,i}^{-2}x^2 + 1)_{i=1}^M$, then $\lim_{x \rightarrow \infty} \mathcal{D}(x)^{-1}x^2 \rightarrow \text{diag}(\omega_{M,i}^2)_{i=1}^M$. By the dual-scale separation hypothesis, $d_{ij} \geq \min(c_1\varepsilon^p, D_{\text{min}})$ for all $i \neq j$. Thus, for any fixed wave speed v and $\varepsilon > 0$, the time delays $\tau_{ij}(\varepsilon) = d_{ij}/v$ are strictly positive constants.

This implies the off-diagonal elements vanish exponentially: $\|\mathcal{D}(x)^{-1}x^2\mathcal{Q}(x, \varepsilon)\| \rightarrow 0$ as $x \rightarrow \infty$. By the continuity of the determinant mapping, we have

$$f(x, \varepsilon) = \det \mathcal{D}(x) \cdot \det \left(I + \mathcal{D}(x)^{-1}x^2\mathcal{Q}(x, \varepsilon) \right) \sim \prod_{i=1}^M (\omega_{M,i}^{-2}x^2 + 1) \neq 0, \quad \text{as } x \rightarrow \infty.$$

By the Identity Theorem (see [1, Ch. 4]), the zero set $Z(\varepsilon) = \{s \in \mathbb{C} : f(s, \varepsilon) = 0\}$ is discrete and has no accumulation points in \mathbb{C} . For $s \in \mathbb{C} \setminus Z(\varepsilon)$, we apply Cramer's rule:

$$P(s, \varepsilon)^{-1} = \frac{\text{adj}(P(s, \varepsilon))}{f(s, \varepsilon)}.$$

Since the entries of $\text{adj}(P(s, \varepsilon))$ are entire functions (being polynomials of the entries of P), $P(s, \varepsilon)^{-1}$ is a matrix of meromorphic functions (see, e.g., [21, Ch. 3]). Given that \mathcal{A}_b , s^2 , and $B^{\text{in}}(s)$ are analytic, their product with $P(s, \varepsilon)^{-1}$ in (5.1) ensures that the transfer matrix $H_b(s, \varepsilon)$ is meromorphic on \mathbb{C} . Finally, in any compact subset of \mathbb{C} , the discreteness of $Z(\varepsilon)$ guarantees at most a finite number of poles.

5.2 Proof of Proposition 2.1(2): Discrete Poles and Asymptotic Cluster Separation

Proof. Let $\mathbb{C}_{\geq 0} = \{s \in \mathbb{C} : \text{Re}(s) \geq 0\}$. The poles of the transfer matrix $H_b(s)$ in the complex plane coincide with the roots of the characteristic equation $F(s, \varepsilon) = 0$, where

$$F(s, \varepsilon) := \det(\mathcal{D}(s) + s^2 \mathcal{Q}(s, \varepsilon)).$$

Here, $\mathcal{D}(s) = \text{diag}(\omega_{M,i}^{-2} s^2 + 1)_{i=1}^M$ represents the unperturbed state, and the physical interaction matrix is $\mathcal{Q}_{ij}(s, \varepsilon) = \varepsilon \frac{\bar{c}_j e^{-s\tau_{ij}}}{4\pi d_{ij}}$ for $i \neq j$. We proceed by establishing the successive claims corresponding to the parts of the proposition.

1. *Claim 1: Near each local Minnaert frequency $i\omega_{M,\alpha}$, there exists a localized collection of exactly M_α poles.*

Define the unperturbed characteristic function:

$$F_0(s) := F(s, 0) = \det(\mathcal{D}(s)) = \prod_{\gamma=1}^N \left(\omega_{M,\gamma}^{-2} s^2 + 1 \right)^{M_\gamma}.$$

The roots of $F_0(s) = 0$ in the upper half-plane are exactly $s = i\omega_{M,\gamma}$ for $\gamma \in \{1, \dots, N\}$, each with algebraic multiplicity M_γ . Because the material properties are distinct between clusters, these roots are strictly separated. For a given cluster α , we define a neighborhood $U_\alpha := \{s \in \mathbb{C} : |s - i\omega_{M,\alpha}| < \rho_\alpha\}$, choosing $\rho_\alpha > 0$ strictly small enough such that $i\omega_{M,\alpha}$ is the unique root of $F_0(s)$ in the closure \bar{U}_α .

By the compactness of ∂U_α , we define the strict minimum $m_\alpha := \min_{s \in \partial U_\alpha} |F_0(s)| > 0$. For the perturbed characteristic function $F(s, \varepsilon) = \det(\mathcal{D}(s) + s^2 \mathcal{Q}(s, \varepsilon))$, we analyze the asymptotic scaling of the matrix norm $\|\mathcal{Q}(s, \varepsilon)\|$ under the dual-scale separation.

- (a) **Intra-cluster terms** ($i, j \in \mathcal{G}_\gamma$): $d_{ij} \geq c_1 \varepsilon^p \implies |\mathcal{Q}_{ij}| = \mathcal{O}(\varepsilon^{1-p})$.
- (b) **Inter-cluster terms** ($i \in \mathcal{G}_\gamma, j \in \mathcal{G}_\beta$): $d_{ij} \geq D_{\min} \implies |\mathcal{Q}_{ij}| = \mathcal{O}(\varepsilon)$.

Because $p \in (0, 1)$, the local intra-cluster interactions dominate as $\varepsilon \rightarrow 0$, yielding a global norm bound $\|\mathcal{Q}(s, \varepsilon)\| = \mathcal{O}(\varepsilon^{1-p})$. Since $1 - p > 0$ and $\sup_{s \in \partial U_\alpha} |s^2| < \infty$, the perturbation vanishes uniformly on the boundary:

$$\lim_{\varepsilon \rightarrow 0} \sup_{s \in \partial U_\alpha} \|s^2 \mathcal{Q}(s, \varepsilon)\| = 0.$$

By the continuity of the determinant mapping, this uniform convergence of the matrix entries implies there exists an $\varepsilon_0 > 0$ such that for all $\varepsilon \in (0, \varepsilon_0)$,

$$\max_{s \in \partial U_\alpha} |F(s, \varepsilon) - F_0(s)| < m_\alpha \leq \min_{s \in \partial U_\alpha} |F_0(s)|.$$

By Rouché's Theorem, this strict inequality on the boundary implies that $F(s, \varepsilon)$ and $F_0(s)$ possess the identical number of roots (counting multiplicities) inside the domain U_α . Since $F_0(s)$ has a root of multiplicity M_α at $i\omega_{M,\alpha}$, we conclude that $F(s, \varepsilon)$ admits a localized cluster of exactly M_α poles inside U_α .

Claim 2: Existence and Dominance of Distinguished Cluster Poles.

Due to macroscopic material detuning between distinct clusters \mathcal{G}_α ($1 \leq \alpha \leq N$), we establish that the local Minnaert poles spectrally split. Let the resonances be the roots of the pencil $P : \mathbb{C} \times \mathbb{R}_{>0} \rightarrow \mathbb{C}^{M \times M}$:

$$P(s, \varepsilon) := \mathcal{D}(s) + s^2 \mathcal{Q}(s, \varepsilon),$$

with $\mathcal{D}(s) := \text{diag}(\omega_{M,i}^{-2} s^2 + 1)_{i=1}^M$ and the interaction matrix elements evaluated near the local resonance $s = i\omega_{M,\alpha}$ given by $\mathcal{Q}_{ij}(i\omega_{M,\alpha}, \varepsilon) := \mathcal{C}_j G(x_i, x_j, i\omega_{M,\alpha})$ for all $i \neq j$. We show that a leading-order block-diagonal decoupling isolates a distinguished simple pole for the dominant principal mode of each cluster:

$$s_{\alpha,1}^* = -\eta_{\alpha,1} + i\omega_{\alpha,1}(\varepsilon), \quad \eta_{\alpha,1}, \omega_{\alpha,1}(\varepsilon) > 0,$$

where $\omega_{\alpha,1}(\varepsilon)$ is the corresponding dominant intra-cluster hybridization shift.

1. Step 1: Multi-Scale Subwavelength Expansion for N Clusters.

Consider N well-separated clusters comprising a total of $M = \sum_{\gamma=1}^N M_\gamma$ bubbles. The inter-bubble distance d_{ij} exhibits a dual-scale geometric separation:

- (a) **Intra-cluster** ($i, j \in \mathcal{G}_\gamma$): $d_{ij} = \tilde{d}_{ij} \varepsilon^p$ for $p \in (0, 1)$.
- (b) **Inter-cluster** ($i \in \mathcal{G}_\gamma, j \in \mathcal{G}_\beta$ with $\gamma \neq \beta$): $d_{ij} = D_{ij} \sim \mathcal{O}(1)$.

Evaluating the free-space Green's function for the global $M \times M$ physical interaction matrix at the local resonance $i\omega_{M,\alpha}$ yields a block-structured multiscale expansion:

$$\mathbf{Q}(i\omega_{M,\alpha}, \varepsilon) = \varepsilon^{1-p} \tilde{\mathbf{C}}^{(0)} - i\varepsilon \mathbf{\Gamma}^{(1)} + \mathcal{O}(\varepsilon^{1+p}),$$

where there exists a permutation matrix $\mathbf{P} \in \{0, 1\}^{M \times M}$ such that the leading-order operator is mapped to a strict direct sum of invariant subspaces:

$$\mathbf{P}^\top \tilde{\mathbf{C}}^{(0)} \mathbf{P} = \bigoplus_{\gamma=1}^N \tilde{C}_\gamma^{(0)} = \text{diag}(\tilde{C}_1^{(0)}, \tilde{C}_2^{(0)}, \dots, \tilde{C}_N^{(0)}). \quad (5.2)$$

Here, each $\tilde{C}_\gamma^{(0)} \in \mathbb{R}^{M_\gamma \times M_\gamma}$ is an irreducible Metzler sub-block.

The perturbation matrix $\mathbf{\Gamma}^{(1)}$ contains both the intra-cluster radiation matrices (in the diagonal blocks) and the macroscopic inter-cluster wave interactions (in the off-diagonal blocks), evaluated at $i\omega_{M,\alpha}$:

$$[\mathbf{\Gamma}^{(1)}]_{\gamma\gamma} = C_\gamma^{(1)}, \quad [\mathbf{\Gamma}^{(1)}]_{\gamma\beta} = iG_{\gamma\beta}(i\omega_{M,\alpha}) \quad (\text{for } \gamma \neq \beta),$$

with $G_{\gamma\beta,ij} = \bar{C}_j \frac{e^{-ik_{M,\alpha} D_{ij}}}{4\pi D_{ij}}$ where the wavenumber is $k_{M,\alpha} = \omega_{M,\alpha}/c_0$.

2. Step 2: Perron-Frobenius Spectrum and Generic Material Detuning.

Since $\tilde{\mathbf{C}}^{(0)}$ is permutation-similar to a block-diagonal matrix, its global spectrum is exactly the union of the individual cluster spectra $\sigma(\tilde{C}_\alpha^{(0)})$ and the global dynamics decouple at $\varepsilon = 0$. Because $\tilde{C}_\alpha^{(0)}$ is non-negative and irreducible, the Perron-Frobenius theorem (see [10, Ch. 8, Th. 8.4.4]) ensures its principal eigenvalue $\tilde{\mu}_{\alpha,1}^{(0)}$ is strictly simple.

Due to Assumption 2(ii), the exact unperturbed global matrix pencil $\mathbf{P}^{(0)}(s)$ at the active resonance $s^{(0)} = i\omega_{M,\alpha}$ yields off-resonant diagonal blocks $\mathbf{P}_{\beta\beta}^{(0)} = \left(1 - \omega_{M,\alpha}^2/\omega_{M,\beta}^2\right) \mathbf{I}_{M_\beta}$. Because the material resonances are strictly disjoint, these macroscopic detuning blocks are strictly invertible. Consequently, the exact unperturbed global principal eigenvectors corresponding to cluster α are rigorously determined as:

$$\mathbf{v}_\alpha^{(0)} = \begin{bmatrix} \mathbf{0} \\ v_{\alpha,1}^{(0)} \\ \mathbf{0} \end{bmatrix}, \quad \mathbf{w}_\alpha^{(0)\top} = \begin{bmatrix} \mathbf{0}^\top & w_{\alpha,1}^{(0)\top} & \mathbf{0}^\top \end{bmatrix} \in \mathbb{R}_{\geq 0}^M,$$

where $v_{\alpha,1}^{(0)}$ and $w_{\alpha,1}^{(0)}$ are the Perron-Frobenius eigenvectors of the active α -block, satisfying the normalization $\mathbf{w}_{\alpha}^{(0)\top} \mathbf{v}_{\alpha}^{(0)} > 0$.

3. Step 3: Kato Analytic Perturbation and Multiscale Projection.

By Kato's analytic perturbation theory for matrix pencils (see [11, Chap. II, Sec. 2.3]), the strictly simple principal eigenvalue $\tilde{\mu}_{\alpha,1}^{(0)}$ of the sub-block $\tilde{\mathbf{C}}_{\alpha}^{(0)}$ ensures the existence of unique, analytic asymptotic branches for the dominant $m = 1$ mode. We denote this perturbed principal pole as $s_{M,\alpha}^*(\varepsilon) = i\omega_{M,\alpha} + \delta(\varepsilon)$ and its corresponding global eigenvector as $\mathbf{v}_{\alpha}(\varepsilon) = \mathbf{v}_{\alpha}^{(0)} + \tilde{\mathbf{v}}(\varepsilon)$. Expanding the non-linear eigenvalue problem $\mathbf{P}(s_{M,\alpha}^*, \varepsilon)\mathbf{v}_{\alpha}(\varepsilon) = 0$ yields:

$$\left[2i\omega_{M,\alpha}^{-1}\delta\mathbf{I} - \omega_{M,\alpha}^2\varepsilon^{1-p}\tilde{\mathbf{C}}^{(0)} + i\omega_{M,\alpha}^2\varepsilon\mathbf{\Gamma}^{(1)} + \omega_{M,\alpha}^{-2}\delta^2\mathbf{I} + \mathcal{O}(\varepsilon^{1+p}) \right] (\mathbf{v}_{\alpha}^{(0)} + \tilde{\mathbf{v}}) = 0.$$

We project this system by left-multiplying with the global left eigenvector $\mathbf{w}_{\alpha}^{(0)\top}$. Because the off-resonant components of both $\mathbf{w}_{\alpha}^{(0)\top}$ and $\mathbf{v}_{\alpha}^{(0)}$ are rigorously zero, this projection perfectly isolates the active block, and this yields:

$$\begin{aligned} \mathbf{w}_{\alpha}^{(0)\top} \tilde{\mathbf{C}}^{(0)} \mathbf{v}_{\alpha}^{(0)} &= \tilde{\mu}_{\alpha,1}^{(0)} \langle w_{\alpha,1}^{(0)}, v_{\alpha,1}^{(0)} \rangle, \\ \mathbf{w}_{\alpha}^{(0)\top} \mathbf{\Gamma}^{(1)} \mathbf{v}_{\alpha}^{(0)} &= w_{\alpha,1}^{(0)\top} [\mathbf{\Gamma}^{(1)}]_{\alpha\alpha} v_{\alpha,1}^{(0)} = w_{\alpha,1}^{(0)\top} C_{\alpha}^{(1)} v_{\alpha,1}^{(0)}. \end{aligned}$$

Imposing Kato's orthogonality condition (see [11, Chap. II, Sec. 3.3]), $\mathbf{w}_{\alpha}^{(0)\top} \tilde{\mathbf{v}} = 0$ strictly bounds the residual projection error to $\mathcal{O}(\delta \cdot \tilde{\mathbf{v}}) \sim \mathcal{O}(\varepsilon^{1+p})$. This prevents collision with the $\mathcal{O}(\varepsilon)$ radiation term, rigorously isolating the characteristic polynomial:

$$2i\omega_{M,\alpha}^{-1}\delta - \omega_{M,\alpha}^2\tilde{\mu}_{\alpha,1}^{(0)}\varepsilon^{1-p} + i\omega_{M,\alpha}^2\mathbf{M}_{11}^{(\alpha)}\varepsilon + \omega_{M,\alpha}^{-2}\delta^2 + \mathcal{O}(\varepsilon^{1+p}) = 0,$$

where the global Rayleigh quotient collapses strictly to the local cluster's radiation projection:

$$\mathbf{M}_{11}^{(\alpha)} := \frac{\mathbf{w}_{\alpha}^{(0)\top} \mathbf{\Gamma}^{(1)} \mathbf{v}_{\alpha}^{(0)}}{\mathbf{w}_{\alpha}^{(0)\top} \mathbf{v}_{\alpha}^{(0)}} = \frac{w_{\alpha,1}^{(0)\top} C_{\alpha}^{(1)} v_{\alpha,1}^{(0)}}{w_{\alpha,1}^{(0)\top} v_{\alpha,1}^{(0)}} \in \mathbb{R}_{>0}.$$

We introduce the asymptotic ansatz for the complex shift $\delta(\varepsilon)$:

$$\delta(\varepsilon) = c_{1-p}\varepsilon^{1-p} + c_{2-2p}\varepsilon^{2-2p} + c_1\varepsilon + \mathcal{O}(\varepsilon^{\min(3-3p, 2-p)}).$$

Balancing the algebraically independent powers of ε yields:

- (a) $\mathcal{O}(\varepsilon^{1-p})$ **Balance:** $c_{1-p} = -i\frac{\omega_{M,\alpha}^3}{2}\tilde{\mu}_{\alpha,1}^{(0)} \in i\mathbb{R}$.
- (b) $\mathcal{O}(\varepsilon^{2-2p})$ **Balance:** $c_{2-2p} = \frac{i}{2\omega_{M,\alpha}}c_{1-p}^2 \in i\mathbb{R}$.
- (c) $\mathcal{O}(\varepsilon^1)$ **Balance:** $c_1 = -\frac{\omega_{M,\alpha}^3}{2}\mathbf{M}_{11}^{(\alpha)} \in \mathbb{R}$.

Defining the perturbed pole as $s_{M,\alpha}^*(\varepsilon) = -\eta_{M,\alpha}(\varepsilon) + i\omega_{M,\alpha}(\varepsilon)$, we separate the real damping and the shifted frequency. The perturbed cluster frequency $\omega_{M,\alpha}(\varepsilon)$ is determined by the imaginary projection of the shift:

$$\omega_{M,\alpha}(\varepsilon) = \omega_{M,\alpha} + \text{Im}(\delta(\varepsilon)) = \omega_{M,\alpha} - \frac{\omega_{M,\alpha}^3}{2}\tilde{\mu}_{\alpha,1}^{(0)}\varepsilon^{1-p} - \frac{\omega_{M,\alpha}^5}{8}(\tilde{\mu}_{\alpha,1}^{(0)})^2\varepsilon^{2-2p} + \mathcal{O}(\varepsilon^{\min(1, 3-3p)}).$$

Correspondingly, the cluster damping $\eta_{M,\alpha}$ is determined by the real projection. Because the lower-order shifts are purely imaginary ($\text{Re}(c_{1-p}) = \text{Re}(c_{2-2p}) = 0$), the leading-order damping is rigorously isolated at $\mathcal{O}(\varepsilon^1)$:

$$\eta_{M,\alpha}(\varepsilon) = -\text{Re}(\delta(\varepsilon)) = \frac{\omega_{M,\alpha}^3}{2}\mathbf{M}_{11}^{(\alpha)}\varepsilon + \mathcal{O}(\varepsilon^{>1}).$$

Consequently, the leading-order damping $\eta_{M,\alpha} = \mathcal{O}(\varepsilon)$ is globally decoupled and inter-cluster terms satisfy $[\mathbf{\Gamma}^{(1)}]_{\alpha\beta} \in \ker(\mathbf{w}_{\alpha}^{(0)\top}(\cdot)\mathbf{v}_{\alpha}^{(0)})$ for all $\alpha \neq \beta$.

4. *Step 4: Pole Simplicity, Spatial Confinement, and Rank-One Residue.*

Assuming the non-degeneracy of $\tilde{\mu}_{\alpha,1}^{(0)}$ (established in Step 2), Kato's perturbation theory implies $s_{M,\alpha}^*(\varepsilon)$ is a strictly simple root of $\det \mathbf{P}(s, \varepsilon) = 0$. Consequently, $\dim \ker \mathbf{P}(s_{M,\alpha}^*, \varepsilon) = 1$, spanned uniquely by the perturbed global eigenvector $\mathbf{v}_\alpha(\varepsilon)$.

Expanding the global resolvent $\mathbf{H}_b(s) = \mathbf{P}(s, \varepsilon)^{-1}$ via the first-order Taylor series of the matrix pencil yields:

$$\mathbf{P}(s, \varepsilon) = \mathbf{P}(s_{M,\alpha}^*, \varepsilon) + (s - s_{M,\alpha}^*) \left. \frac{\partial \mathbf{P}}{\partial s} \right|_{s_{M,\alpha}^*} + \mathcal{O}((s - s_{M,\alpha}^*)^2). \quad (5.3)$$

The projection onto the 1D kernel defines the rank-one global residue $\mathcal{R}_{M,\alpha}$:

$$\mathcal{R}_{M,\alpha} = \lim_{s \rightarrow s_{M,\alpha}^*} (s - s_{M,\alpha}^*) \mathbf{P}(s, \varepsilon)^{-1} = \frac{\mathbf{v}_\alpha(\varepsilon) \mathbf{w}_\alpha(\varepsilon)^\top}{\mathbf{w}_\alpha(\varepsilon)^\top \left. \frac{\partial \mathbf{P}}{\partial s} \right|_{s_{M,\alpha}^*} \mathbf{v}_\alpha(\varepsilon)}. \quad (5.4)$$

The denominator (the generalized Jacobian $\mathbf{J}_\alpha(\varepsilon)$) evaluates the operator's transversality at the pole. Consistent with the unperturbed block-diagonal pencil $\mathbf{P}_{\alpha\alpha}^{(0)}(s) = (1 + s^2/\omega_{M,\alpha}^2) \mathbf{I}$ defined in Step 3, the local derivative is $\left. \frac{\partial \mathbf{P}}{\partial s} \right|_{s_{M,\alpha}^*} \approx \frac{2s}{\omega_{M,\alpha}^2} \mathbf{I}$. Applying the multiscale shifts $s_{M,\alpha}^* = i\omega_{M,\alpha} + \mathcal{O}(\varepsilon^{1-p})$ and $\mathbf{v}_\alpha(\varepsilon) = \mathbf{v}_\alpha^{(0)} + \mathcal{O}(\varepsilon^{1-p})$ yields:

$$\mathbf{J}_\alpha(\varepsilon) = \mathbf{w}_\alpha^{(0)\top} \left(\frac{2i}{\omega_{M,\alpha}} \mathbf{I} \right) \mathbf{v}_\alpha^{(0)} + \mathcal{O}(\varepsilon^{1-p}) = \frac{2i}{\omega_{M,\alpha}} \langle w_{\alpha,1}^{(0)}, v_{\alpha,1}^{(0)} \rangle + \mathcal{O}(\varepsilon^{1-p}). \quad (5.5)$$

Because the unperturbed eigenvectors $\mathbf{v}_\alpha^{(0)}$ and $\mathbf{w}_\alpha^{(0)}$ are rigorously zero outside the active cluster index set \mathcal{I}_α , their outer product $\mathbf{v}_\alpha^{(0)} \mathbf{w}_\alpha^{(0)\top}$ is strictly block-sparse. To leading multiscale order, $\mathcal{R}_{M,\alpha}$ is confined strictly to the $\alpha \times \alpha$ principal block:

$$\mathcal{R}_{M,\alpha} \approx \frac{\omega_{M,\alpha}}{2i \langle w_{\alpha,1}^{(0)}, v_{\alpha,1}^{(0)} \rangle} \begin{bmatrix} \mathbf{0} & \mathbf{0} & \mathbf{0} \\ \mathbf{0} & v_{\alpha,1}^{(0)} w_{\alpha,1}^{(0)\top} & \mathbf{0} \\ \mathbf{0} & \mathbf{0} & \mathbf{0} \end{bmatrix}. \quad (5.6)$$

This guarantees rigorous spatial confinement: near resonance, the rank-one resolvent operator maps any global incident field solely onto cluster α 's principal in-phase mode.

Finally, the half-power bandwidth Γ_α is strictly determined by the pole's real part, $\text{Re}(s_{M,\alpha}^*) = -\eta_{M,\alpha}$. From Step 3, the bandwidth is rigorously isolated at $\mathcal{O}(\varepsilon)$:

$$\Gamma_\alpha = 2|\text{Re}(s_{M,\alpha}^*)| = 2\eta_{M,\alpha} = \omega_{M,\alpha}^3 \mathbf{M}_{11}^{(\alpha)} \varepsilon + \mathcal{O}(\varepsilon^{>1}). \quad (5.7)$$

5. *Step 5: For each cluster $\alpha \in \{1, \dots, N\}$, the distinguished pole $s_{M,\alpha}^*(\varepsilon) = -\eta_{M,\alpha}(\varepsilon) + i\omega_{M,\alpha}(\varepsilon)$ satisfies $\eta_{M,\alpha} > 0$ for $\varepsilon > 0$.*

We investigate the stability of the distinguished pole $s_{M,\alpha}^*(\varepsilon)$ by analyzing the operator in the neighborhood of $s^{(0)} = i\omega_{M,\alpha}$. As rigorously isolated in Step 3, the leading-order damping is governed by:

$$\eta_{M,\alpha} = \varepsilon \frac{\omega_{M,\alpha}^3}{2} \mathbf{M}_{11}^{(\alpha)} + \mathcal{O}(\varepsilon^{>1}), \quad \mathbf{M}_{11}^{(\alpha)} = \frac{\mathbf{w}_\alpha^{(0)\top} \mathbf{\Gamma}^{(1)} \mathbf{v}_\alpha^{(0)}}{\mathbf{w}_\alpha^{(0)\top} \mathbf{v}_\alpha^{(0)}}, \quad (5.8)$$

where $\mathbf{\Gamma}^{(1)} := -\text{Im}[\mathbf{Q}(i\omega_{M,\alpha})] = \frac{\bar{C}_j \sin(k_{M,\alpha} d_{ij})}{4\pi d_{ij}}$ is the global radiation matrix. To prove $\eta_{M,\alpha} > 0$, we establish that \mathbf{A} is strictly positive definite ($\mathbf{\Gamma}^{(1)} \succ 0$). Using the identity $\frac{\sin(k|x-y|)}{k|x-y|} =$

$\frac{1}{4\pi} \int_{\mathbb{S}^2} e^{ik\hat{d}\cdot(x-y)} d\Omega(\hat{d})$, and noting that $\mathbf{v}_\alpha^{(0)}$ has strictly zero entries outside the index set \mathcal{G}_α , the power integral collapses locally to cluster α as follows:

$$\begin{aligned} \mathbf{v}_\alpha^{(0)*} \mathbf{\Gamma}^{(1)} \mathbf{v}_\alpha^{(0)} &= \overline{C}_j \sum_{i,j \in \mathcal{G}_\alpha} \overline{v}_{\alpha,i}^{(0)} v_{\alpha,j}^{(0)} \left[\frac{k_{M,\alpha}}{(4\pi)^2} \int_{\mathbb{S}^2} e^{ik_{M,\alpha}\hat{d}\cdot x_i} e^{-ik_{M,\alpha}\hat{d}\cdot x_j} d\Omega \right] \\ &= \overline{C}_j \frac{k_{M,\alpha}}{(4\pi)^2} \int_{\mathbb{S}^2} \left(\sum_{i \in \mathcal{G}_\alpha} \overline{v}_{\alpha,i}^{(0)} e^{ik_{M,\alpha}\hat{d}\cdot x_i} \right) \left(\sum_{j \in \mathcal{G}_\alpha} v_{\alpha,j}^{(0)} e^{-ik_{M,\alpha}\hat{d}\cdot x_j} \right) d\Omega \\ &= \overline{C}_j \frac{k_{M,\alpha}}{(4\pi)^2} \int_{\mathbb{S}^2} \left| \sum_{j \in \mathcal{G}_\alpha} v_{\alpha,j}^{(0)} e^{-ik_{M,\alpha}\hat{d}\cdot x_j} \right|^2 d\Omega \geq 0. \end{aligned} \quad (5.9)$$

Assume $\mathbf{v}_\alpha^{(0)*} \mathbf{\Gamma}^{(1)} \mathbf{v}_\alpha^{(0)} = 0$. By the non-negativity of the integrand, the acoustic far-field pattern $\mathcal{F}_\alpha(\hat{d}) = \sum_{j \in \mathcal{G}_\alpha} v_{\alpha,j}^{(0)} e^{-ik_{M,\alpha}\hat{d}\cdot x_j}$ must vanish identically for all $\hat{d} \in \mathbb{S}^2$. By Rellich's Lemma, the corresponding acoustic field $u(x) = \sum_{j \in \mathcal{G}_\alpha} v_{\alpha,j}^{(0)} \frac{e^{ik_{M,\alpha}|x-x_j|}}{4\pi|x-x_j|}$ must satisfy $u(x) \equiv 0$ in the exterior domain $\mathbb{R}^3 \setminus \text{conv}\{x_j\}_{j \in \mathcal{G}_\alpha}$.

By the Unique Continuation Principle, $u(x) = 0$ for all $x \in \mathbb{R}^3 \setminus \{x_j\}_{j \in \mathcal{G}_\alpha}$. In the sense of distributions:

$$(\Delta + k_{M,\alpha}^2)u = - \sum_{j \in \mathcal{G}_\alpha} v_{\alpha,j}^{(0)} \delta(x - x_j) = 0. \quad (5.10)$$

Since the mesoscale positions $\{x_j\}_{j \in \mathcal{G}_\alpha}$ are spatially distinct, the linear independence of the Dirac measures necessitates that the local coefficients $v_{\alpha,j}^{(0)} = 0$ for all $j \in \mathcal{G}_\alpha$, implying the local eigenvector $v_{\alpha,1}^{(0)} = \mathbf{0}$. This directly contradicts the Perron-Frobenius theorem (Step 2), which guarantees $v_{\alpha,1}^{(0)} \in \mathbb{R}_{>0}^{M_\alpha}$.

It immediately follows that the Kato radiation quotient is strictly positive ($\mathbf{M}_{11}^{(\alpha)} > 0$), yielding:

$$\eta_{M,\alpha} = \frac{\omega_{M,\alpha}^3}{2} \mathbf{M}_{11}^{(\alpha)} \varepsilon + \mathcal{O}(\varepsilon^{>1}) > 0 \quad (5.11)$$

for sufficiently small $\varepsilon > 0$. The distinguished pole for each cluster is rigorously stable.

6. Step 6: Existence of a Strictly Positive Spectral Gap $g(\varepsilon)$.

Let $\mathcal{P}(\varepsilon) \subset \mathbb{C}$ denote the discrete poles of the global resolvent $\mathbf{H}_b(s, \varepsilon)$. We define the ε -dependent neighborhood $U_\alpha(\varepsilon) := \{s \in \mathbb{C} : |s - s_{M,\alpha}^*| < c\varepsilon^{1-p}\}$ for a sufficiently small constant $c > 0$.

Let $\mathcal{P}_{\text{out}}(\varepsilon) := \mathcal{P}(\varepsilon) \setminus \{s_{M,\alpha}^*(\varepsilon)\}$. Due to Step 2, the generic disjointness ($\omega_{M,\alpha} \neq \omega_{M,\beta}$), guarantees distinct cluster principle dominant poles are strictly isolated by an $\mathcal{O}(1)$ spectral distance, quantified as:

$$|s_{M,\alpha}^*(\varepsilon) - s_{M,\beta}^*(\varepsilon)| = |\omega_{M,\alpha} - \omega_{M,\beta}| + \mathcal{O}(\varepsilon^{1-p}) \geq \Delta_\omega > 0, \quad (5.12)$$

where $\Delta_\omega := \frac{1}{2} \min_{\omega_{M,\beta} \neq \omega_{M,\alpha}} |\omega_{M,\alpha} - \omega_{M,\beta}|$.

Conversely, for higher-order intra-cluster modes sharing the same unperturbed local frequency $\omega_{M,\alpha}$, the simplicity of the Perron-Frobenius eigenvalue guarantees a strict local intra-cluster gap:

$$\Delta_{\text{gap}} := \text{dist} \left(\tilde{\mu}_{\alpha,1}^{(0)}, \sigma(\tilde{\mathbf{C}}_\alpha^{(0)}) \setminus \{\tilde{\mu}_{\alpha,1}^{(0)}\} \right) > 0.$$

By the asymptotic expansion of the pole shifts (Step 3), the constant c can be chosen small enough such that $\mathcal{P}_{\text{out}}(\varepsilon) \cap \bar{U}_\alpha(\varepsilon) = \emptyset$ for all $\varepsilon \in (0, \varepsilon_0]$. Given the closedness of $\mathcal{P}_{\text{out}}(\varepsilon)$, we define the isolation gap:

$$g(\varepsilon) := \text{dist}(s_{M,\alpha}^*(\varepsilon), \mathcal{P}_{\text{out}}(\varepsilon)) > 0, \quad \forall \varepsilon \in (0, \varepsilon_0]. \quad (5.13)$$

Consequently, the generic disjointness ensures a strictly positive, asymptotically scaled lower bound $g(\varepsilon) \geq g_0 \varepsilon^{1-p} > 0$ for some constant $g_0 > 0$. Thus, for $\varepsilon > 0$, the spatially localized resonance pole $s_{M,\alpha}^*(\varepsilon)$ remains rigorously isolated from the complementary spectrum.

5.3 Proof of Proposition 2.1(3): Residue Expansion at the Distinguished Pole

3. *Proof of Proposition 2.1(3).* The global transfer function $H_b(s, \varepsilon) = \mathcal{A}_b \mathbf{P}(s, \varepsilon)^{-1} s^2 \mathbf{B}^{\text{in}}(s)$ is meromorphic. By Step 4, the resolvent $\mathbf{P}(s, \varepsilon)^{-1}$ exhibits a simple pole at $s_{M, \alpha}^*(\varepsilon)$ with the rank-one global residue $\mathcal{R}_{M, \alpha}(\varepsilon) = \mathbf{v}_\alpha(\varepsilon) \mathbf{w}_\alpha(\varepsilon)^\top / \mathcal{G}_\alpha(\varepsilon)$. Since the observation operator \mathcal{A}_b is linear and the excitation $s^2 \mathbf{B}^{\text{in}}(s)$ is analytic near $s_{M, \alpha}^*(\varepsilon)$, $H_b(s, \varepsilon)$ admits the Laurent expansion:

$$H_b(s, \varepsilon) = \frac{R_{M, \alpha}(\varepsilon)}{s - s_{M, \alpha}^*(\varepsilon)} + H_{\text{reg}}(s, \varepsilon), \quad (5.14)$$

where H_{reg} is analytic on a punctured neighborhood of $s_{M, \alpha}^*(\varepsilon)$. Evaluating the limit $s \rightarrow s_{M, \alpha}^*(\varepsilon)$ isolates the scalar observable residue $R_{M, \alpha}(\varepsilon)$:

$$R_{M, \alpha}(\varepsilon) = \mathcal{A}_b \mathcal{R}_{M, \alpha}(\varepsilon) (s_{M, \alpha}^*(\varepsilon))^2 \mathbf{B}^{\text{in}}(s_{M, \alpha}^*(\varepsilon)) = \frac{(s_{M, \alpha}^*(\varepsilon))^2}{\mathcal{G}_\alpha(\varepsilon)} [\mathcal{A}_b \mathbf{v}_\alpha(\varepsilon)] \left[\mathbf{w}_\alpha(\varepsilon)^\top \mathbf{B}^{\text{in}}(s_{M, \alpha}^*(\varepsilon)) \right]. \quad (5.15)$$

Substituting the asymptotic limits established in Steps 3 and 4 yields $(s_{M, \alpha}^*(\varepsilon))^2 = -\omega_{M, \alpha}^2 + \mathcal{O}(\varepsilon^{1-p})$ and the corrected operator transversality $\mathcal{G}_\alpha(\varepsilon) = \frac{2i}{\omega_{M, \alpha}} \langle w_{\alpha, 1}^{(0)}, v_{\alpha, 1}^{(0)} \rangle + \mathcal{O}(\varepsilon^{1-p})$. The multiscale geometric confinement ensures $\mathbf{v}_\alpha(\varepsilon) \approx \mathbf{v}_\alpha^{(0)}$ and $\mathbf{w}_\alpha(\varepsilon) \approx \mathbf{w}_\alpha^{(0)}$, which are supported strictly on the cluster index set \mathcal{I}_α . Thus, the non-annihilation condition is mathematically equivalent to strictly positive macroscopic coupling to the specific cluster's in-phase monopole mode: $\mathcal{A}_b \mathbf{v}_\alpha^{(0)} \neq 0$ and $\mathbf{w}_\alpha^{(0)\top} \mathbf{B}^{\text{in}}(i\omega_{M, \alpha}) \neq 0$. Consequently, the leading-order expansion evaluates to:

$$R_{M, \alpha}(\varepsilon) = \frac{i\omega_{M, \alpha}^3}{2\langle w_{\alpha, 1}^{(0)}, v_{\alpha, 1}^{(0)} \rangle} \left[\mathcal{A}_b \mathbf{v}_\alpha^{(0)} \right] \left[\mathbf{w}_\alpha^{(0)\top} \mathbf{B}^{\text{in}}(i\omega_{M, \alpha}) \right] + \mathcal{O}(\varepsilon^{1-p}) \neq 0. \quad (5.16)$$

Therefore, $R_{M, \alpha}(\varepsilon)$ is strictly non-vanishing for sufficiently small $\varepsilon > 0$, formally establishing the cluster-localized $s_{M, \alpha}^*(\varepsilon)$ as a dominant, physically observable macroscopic singularity.

Remark 5.1. Throughout Section 6.3 spectral bands such as J and I_M are subsets of the frequency axis for the Fourier variable ω . When working in the Laplace domain we evaluate the resolvent along vertical lines $s = \sigma + i\omega$ with fixed $\sigma > 0$ and $\omega \in J$. Thus, although the analysis is carried out in the Laplace variable s , the notion of “frequency band” always refers to the imaginary part ω .

6 Resonant Gain and Approximate Surjectivity

Having derived the Laplace-domain transfer matrices in the previous section, we now connect them to the time-domain physical bubble model. The point of this section is to distinguish formal realization from efficient physical realization by exterior incident waves. Away from the Minnaert bands the inverse actuator map may exist but its norm diverges as the bubble size tends to zero; on the separated Minnaert bands the resonant gain compensates the small capacitance scaling and yields uniformly controlled exterior transducer amplitudes.

6.1 The Actuator Map and Band-Pass Filtering

Let $\{x_m^{\text{tr}}\}_{m=1}^{M_{\text{tr}}} \subset \mathbb{R}^3 \setminus \bar{\Omega}$ denote the exterior transducer locations. For a fixed horizon $T > 0$, we define the physical transducer input space and the macroscopic cluster-source space as

$$U_{\text{tr}} := \{ \boldsymbol{\lambda} \in H^2(0, T; \mathbb{R}^{M_{\text{tr}}}) : \boldsymbol{\lambda}(0) = \dot{\boldsymbol{\lambda}}(0) = \mathbf{0} \}, \quad V := H^1(0, T; \mathbb{R}^N).$$

The H^2 -regularity of U_{tr} guarantees that the delayed incident traces satisfy $\mathbf{u}^{\text{in}}(z_i, \cdot) \in H^2(0, T)$, ensuring the microscopic bubble dynamics are driven by $L^2(0, T)$ accelerations $\partial_t^2 \mathbf{u}^{\text{in}}(z_i, \cdot)$.

The full physical actuator map $\mathcal{F}^\varepsilon \in \mathcal{L}(U_{\text{tr}}, V)$, mapping $\boldsymbol{\lambda} \mapsto \mathbf{q}_{\text{cl}}^\varepsilon$, admits the time-domain compositional structure:

$$\boldsymbol{\lambda} \xrightarrow{G_{\text{tr}}} \mathbf{u}^{\text{in}} \Big|_{\{z_i\}_{i=1}^M} \xrightarrow{H_b} \mathbf{q} \xrightarrow{B_{\text{out}}} \mathbf{q}_{\text{cl}}^\varepsilon.$$

In the Laplace domain, this corresponds exactly to the algebraic factorization of the exterior-to-cluster transfer matrix:

$$\mathcal{H}_{\text{ext}}^\varepsilon(s) = B_{\text{out}} H_b(s) G_{\text{tr}}(s) \in \mathbb{C}^{N \times M_{\text{tr}}}. \quad (6.1)$$

For spectral localization, let $E_T : L^2(0, T; \mathbb{R}^m) \rightarrow L^2(\mathbb{R}; \mathbb{R}^m)$ be the zero-extension operator, and \mathcal{F} the Fourier transform. Given a bounded frequency band J , let $\chi_J \in C_c^\infty(\mathbb{R})$ be a smooth cutoff satisfying $\chi_J \equiv 1$ on J with $\text{supp } \chi_J \subset J_+$ for a slightly larger open interval J_+ . The band-pass projection $\Pi_J : V \rightarrow V$ is defined by

$$\Pi_J \mathbf{w} := \left(\mathcal{F}^{-1}(\chi_J \mathcal{F}(E_T \mathbf{w})) \right) \Big|_{(0, T)}.$$

We define the associated finite-time band-limited source space as

$$V_J := \text{Ran}(\Pi_J) \subset V.$$

Because χ_J is compactly supported, the Paley-Wiener theorem implies that the filtered signals are smooth in time. Consequently, V_J embeds continuously into $H^s(0, T; \mathbb{R}^N)$ for all $s \geq 0$, with embedding constants depending solely on the support of J .

6.2 Asymptotic Divergence and Control Constraints on Non-Resonant Bands

By definition, the effective sources are $q_i^\varepsilon(t) = -C_i(\varepsilon) \tilde{Y}_i(t)$, where the capacitance scales as $C_i(\varepsilon) = \varepsilon \tilde{C}_i$. Thus, the mapping $\tilde{Y} \mapsto q^\varepsilon$ carries an explicit geometric attenuation factor ε . We now quantify the consequence of this scaling on generic, non-resonant bands.

Let $J \subset (0, \infty)$ be a compact interval and define the spectral contour $\Gamma_J := \{i\omega : \omega \in J\} \subset i\mathbb{R}$. Let d_J denote the minimal distance from Γ_J to the pole set $\mathcal{P} = \{s_j^*\}$ of the transfer matrix H_b :

$$d_J := \inf_{\omega \in J, s_j^* \in \mathcal{P}} |i\omega - s_j^*| > 0.$$

Proposition 6.1 (Non-resonant bands: asymptotically small gain). *Considering the fact $d_J > 0$, under the asymptotic scaling $C_i(\varepsilon) = \varepsilon \tilde{C}_i$, there exists a constant $C_J > 0$ independent of ε such that the transfer matrix satisfies:*

$$\sup_{\omega \in J} \|H_b(i\omega)\|_{\mathcal{L}(\mathbb{C}^M, \mathbb{C}^M)} \leq \varepsilon \frac{C_J}{d_J}. \quad (6.2)$$

Furthermore, if $H_b(i\omega)$ admits a measurable right inverse $H_b(i\omega)^\#$, its operator norm strictly diverges as $\varepsilon \rightarrow 0$:

$$\text{ess sup}_{\omega \in J} \|H_b(i\omega)^\#\| \geq \frac{1}{\sup_{\omega \in J} \|H_b(i\omega)\|} \geq \frac{d_J}{\varepsilon C_J}.$$

Proof. By Proposition 2.1, H_b is meromorphic in $\mathcal{S}_{-\sigma_0}$. The scaling $C_i(\varepsilon) = \varepsilon \tilde{C}_i$ implies the bubble capacitance matrix scales linearly as $C^\varepsilon = \varepsilon \tilde{C}$. Now, by the linearity of monopole coupling in the subwavelength limit, $H_b(s)$ admits the factorization:

$$H_b(s) = \varepsilon \tilde{H}_b(s),$$

where $\tilde{H}_b(s)$ is a meromorphic matrix independent of ε and inherits the identical pole structure $\{s_j^*\}$. Applying standard resolvent estimates for meromorphic matrices (see, e.g., [22]), there exists a uniform constant $C > 0$ such that for any $s \in \mathbb{C} \setminus \mathcal{P}$:

$$\|\tilde{H}_b(s)\| \leq \frac{C}{\text{dist}(s, \mathcal{P})}.$$

Restricting this estimate to the imaginary axis $s = i\omega$ for $\omega \in J$, where $\text{dist}(i\omega, \mathcal{P}) \geq d_J$ by definition, we obtain $\|\tilde{H}_b(i\omega)\| \leq C_J/d_J$. Substitution into the factorization yields the upper bound in (6.2).

The lower bound on the right inverse follows algebraically from the sub-multiplicativity of the induced operator norm: $\|I\| \leq \|H_b(i\omega)\| \|H_b(i\omega)^\#\|$. ■

The Divergence Problem: Proposition 6.1 rigorously establishes that actuation on a non-resonant band is asymptotically ill-conditioned. Producing an $\mathcal{O}(1)$ ideal source profile $q^{\text{ideal}} \in V_J$ requires an incident tracking field $\lambda^\varepsilon \in U_{\text{tr}}$ whose physical control cost scales as $\|\lambda^\varepsilon\|_{U_{\text{tr}}} \geq \mathcal{O}(\varepsilon^{-1})$. As $\varepsilon \rightarrow 0$, realizing the ideal control away from resonance requires infinite energy.

6.3 Approximate Surjectivity on the Minnaert Band

To bypass the divergence obstacle, we restrict our target tracking to the composite Minnaert band $I_M := \bigcup_{\alpha=1}^N I_\alpha(\varepsilon)$, where $I_\alpha(\varepsilon) = [\hat{\omega}_{\tau(\alpha)} - \delta(\varepsilon), \hat{\omega}_{\tau(\alpha)} + \delta(\varepsilon)]$. For each cluster α , the local spectral contour passes near its principal perturbed Minnaert pole $s_{M,\alpha}^* = -\eta_\alpha + i\hat{\omega}_{\tau(\alpha)}$.

Proposition 6.2 (Composite Minnaert band: local expansion and resonant gain). *Given the pole structure of $H_b(s)$ and the capacity scaling $C_i(\varepsilon) = \varepsilon\tilde{C}_i$, there exist uniform constants $C_1, C_2 > 0$ such that for any local band $I_\alpha(\varepsilon) \subset I_M$, the transfer matrix admits the local Laurent expansion:*

$$H_b(i\omega) = \frac{R_\alpha}{i\omega - s_{M,\alpha}^*} + H_{\text{reg},\alpha}(i\omega), \quad \omega \in I_\alpha(\varepsilon),$$

where $R_\alpha = \varepsilon\tilde{R}_\alpha$ and $H_{\text{reg},\alpha} = \varepsilon\tilde{H}_{\text{reg},\alpha}$ are $\mathcal{O}(\varepsilon)$. Specifically, with $|i\omega - s_{M,\alpha}^*| = \sqrt{(\omega - \hat{\omega}_{\tau(\alpha)})^2 + \eta_\alpha^2}$, we have:

$$\|H_{\text{reg},\alpha}(i\omega)\| \leq \varepsilon C_1, \quad \frac{\varepsilon}{C_2 |i\omega - s_{M,\alpha}^*|} \leq \left\| \frac{R_\alpha}{i\omega - s_{M,\alpha}^*} \right\| \leq \frac{\varepsilon C_2}{|i\omega - s_{M,\alpha}^*|}.$$

Consequently, defining $\eta_{\min} := \min_\alpha \eta_\alpha$ and $\eta_{\max} := \max_\alpha \eta_\alpha$, there exist uniform constants $c_1, c_2 > 0$ yielding the composite resonant gain on I_M :

$$c_1 \frac{\varepsilon}{\eta_{\max}} \leq \sup_{\omega \in I_M} \|H_b(i\omega)\| \leq c_2 \frac{\varepsilon}{\eta_{\min}}. \quad (6.3)$$

Proof. For any $\omega \in I_M$, there exists a unique $\alpha \in \{1, \dots, N\}$ such that $\omega \in I_\alpha(\varepsilon)$ due to the spectral isolation (Assumption 2.2). The scaling $C_i(\varepsilon) = \varepsilon\tilde{C}_i$ implies the global factorization $H_b(s) = \varepsilon\tilde{H}_b(s)$. Expanding $\tilde{H}_b(s)$ locally near $s_{M,\alpha}^*$ yields $\tilde{H}_b(s) = \frac{\tilde{R}_\alpha}{s - s_{M,\alpha}^*} + \tilde{H}_{\text{reg},\alpha}(s)$. The norm bounds follow since \tilde{R}_α has finite rank and nonzero singular values, and $\tilde{H}_{\text{reg},\alpha}$ is analytic on $I_\alpha(\varepsilon)$. By the reverse triangle inequality locally on $I_\alpha(\varepsilon)$:

$$\|H_b(i\omega)\| \geq \left\| \frac{R_\alpha}{i\omega - s_{M,\alpha}^*} \right\| - \|H_{\text{reg},\alpha}(i\omega)\| \geq \frac{\varepsilon}{C_2 \sqrt{(\omega - \hat{\omega}_{\tau(\alpha)})^2 + \eta_\alpha^2}} - \varepsilon C_1.$$

Evaluating at the exact local resonance ($\omega = \hat{\omega}_{\tau(\alpha)}$) yields $\|H_b(i\hat{\omega}_{\tau(\alpha)})\| \geq \frac{\varepsilon}{C_2 \eta_\alpha} - \varepsilon C_1$. Taking the supremum over all local bands gives the global lower bound. Conversely, the standard triangle inequality on each $I_\alpha(\varepsilon)$ provides the local upper bound $\leq \frac{\varepsilon C_2}{\eta_\alpha} + \varepsilon C_1$. Taking the maximum over all α yields the global upper bound bounded by $\mathcal{O}(\varepsilon/\eta_{\min})$. ■

Proposition 6.3 (Right inverses for the exterior-to-cluster map). *Let $J \subset (0, \infty)$ be compact, and let*

$$H_b : J \rightarrow \mathbb{C}^{N \times M_{\text{tr}}}$$

be continuous. Due to the estimate in (2.20), we have

$$\sigma_*(J) := \inf_{\omega \in J} \sigma_{\min}(H_b(\omega)) > 0. \quad (6.4)$$

Then $H_b(\omega)$ has full row rank N for every $\omega \in J$ and admits the Moore–Penrose right inverse $H(\omega)^\dagger$ satisfying

$$H_b(\omega)H_b(\omega)^\dagger = I_N, \quad \sup_{\omega \in J} \|H_b(\omega)^\dagger\| \leq \sigma_*(J)^{-1}.$$

Conversely, any uniformly bounded measurable right inverse gives a positive lower bound on $\sigma_(J)$.*

Proof. This is the standard singular-value characterization of surjectivity for rectangular matrices. Full row rank is equivalent to positivity of the smallest row singular value, and the Moore–Penrose inverse has norm equal to its reciprocal. ■

Proposition 6.4 (Composite Minnaert-band exterior right inverse). *Recall that $I_M = \bigcup_{\alpha=1}^N I_\alpha(\varepsilon)$ is the separated union of the local Minnaert bands. Assume the macroscopic transducer accessibility condition established in Section 1.6 (Assumption 3) and the microscopic dominant-cluster residue structure supplied by Proposition 6.2. Then the exterior-to-cluster transfer matrix $\mathcal{H}_{\text{ext}}^\varepsilon(i\omega)$ has full row rank N for all $\omega \in I_M$ and admits a right inverse satisfying*

$$\sup_{\omega \in I_M} \left\| \left(\mathcal{H}_{\text{ext}}^\varepsilon(i\omega) \right)^\dagger \right\| \leq C \frac{\eta_{\max}}{\varepsilon}. \quad (6.5)$$

In particular, since the radiation damping scales as $\eta_{\max} = \mathcal{O}(\varepsilon)$, the right inverse from exterior transducer amplitudes to effective cluster-source strengths is uniformly bounded in the Minnaert regime.

Proof. In the frequency domain, the full physical transmission operator corresponds to the factorization

$$\mathcal{H}_{\text{ext}}^\varepsilon(i\omega) = B_{\text{out}} H_b(i\omega) G_{\text{tr}}(i\omega).$$

Combining the geometric full-rank property of the boundary trace matrix G_{tr} with the local resonant amplification of $H_b(i\omega)$ established in Proposition 6.2 immediately yields the lower singular-value estimate formalized in Section 2.3:

$$\sigma_{\min}(\mathcal{H}_{\text{ext}}^\varepsilon(i\omega)) \geq c_{\text{ext}} \frac{\varepsilon}{\eta_{\max}}, \quad \omega \in I_M.$$

Applying the rectangular right-inverse bound from Proposition 6.3 directly to this lower singular-value estimate yields (6.5). Uniform boundedness follows immediately from the linear damping scale $\eta_{\max} = \mathcal{O}(\varepsilon)$. \blacksquare

Remark 6.5 (Minnaert vs. non-resonant efficiency). *Propositions 6.1 and 6.4 establish a sharp physical and mathematical contrast via the ε -scaling:*

1. *Non-resonant band J (where $\text{dist}(J, \{s_m^*\}) \geq d_J > 0$):*

$$\sup_{\omega \in J} \|H_b(i\omega)\| = \mathcal{O}\left(\frac{\varepsilon}{d_J}\right).$$

If the exact inverse exists, its physical cost is strictly bounded from below: $\sup_{\omega \in J} \|H_b^{-1}(i\omega)\| \geq \mathcal{O}\left(\frac{d_J}{\varepsilon}\right)$.

2. *Composite Minnaert band I_M (with local cluster dampings $\eta_\alpha > 0$):*

$$\sup_{\omega \in I_M} \|H_b(i\omega)\| = \mathcal{O}\left(\frac{\varepsilon}{\eta_{\min}}\right).$$

If the compressed exterior-to-cluster map $\mathcal{H}_{\text{ext}}^\varepsilon(i\omega)$ satisfies the exterior-to-cluster lower singular-value condition (2.20), then it admits a uniformly bounded right inverse on the entire composite band. More precisely, its physical control cost is $\mathcal{O}(\eta_{\max}/\varepsilon)$, which is $\mathcal{O}(1)$ because $\eta_{\max} = \mathcal{O}(\varepsilon)$.

Physical Conclusion: The composite Minnaert resonance transforms the bubble clusters into highly efficient actuators. Realizing a target cluster-source profile q^ε through exterior transducers requires a control cost proportional to $\mathcal{O}(\eta_{\max}/\varepsilon)$, reducing the required effort by a massive factor of $\mathcal{O}(\eta_{\max}/d_J)$ compared to the non-resonant regime. In the unphysical, undamped limit ($\eta_{\max} \rightarrow 0$), this gain diverges, and a uniformly bounded exact inverse on I_M ceases to exist.

We now rigorously prove that on the Minnaert band I_M , the actuator map admits a uniformly bounded right inverse.

Proposition 6.6 (Uniform surjectivity on the Minnaert band). *Let $I_M \subset (0, \infty)$ be the bounded composite interval defined by $I_M := \bigcup_{\alpha=1}^N I_\alpha(\varepsilon)$ and let $T > 0$ be fixed. There exist $\varepsilon_0 > 0$, $\beta > 0$, $C_T > 0$, and a family of uniformly bounded linear right-inverse operators*

$$R_{I_M}^\varepsilon : V_{I_M} \rightarrow U_{\text{tr}}, \quad 0 < \varepsilon < \varepsilon_0,$$

such that, for all $q^{\text{ideal}} \in V_{I_M}$ and $0 < \varepsilon < \varepsilon_0$,

$$\left\| \mathcal{F}^\varepsilon R_{I_M}^\varepsilon q^{\text{ideal}} - q^{\text{ideal}} \right\|_V \leq C_T \varepsilon^\beta \left\| q^{\text{ideal}} \right\|_V. \quad (6.6)$$

Crucially, the physical control cost is uniformly bounded: $\|R_{I_M}^\varepsilon\|_{\mathcal{L}(V_{I_M}, U_{\text{tr}})} = \mathcal{O}(1)$ as $\varepsilon \rightarrow 0$.

Proof. By the Fourier isomorphism $\mathcal{F} : L^2(\mathbb{R}_t) \rightarrow L^2(\mathbb{R}_\omega)$, the principal part of the actuator map \mathcal{F}^ε restricted to V_{I_M} is equivalent to the frequency-domain multiplication operator $S_{I_M} \in \mathcal{L}(L^2(I_M; \mathbb{C}^{M_{\text{tr}}}), L^2(I_M; \mathbb{C}^N))$ defined by:

$$(S_{I_M} \widehat{\lambda})(i\omega) := \mathcal{H}_{\text{ext}}^\varepsilon(i\omega) \widehat{\lambda}(i\omega), \quad \omega \in I_M.$$

On the composite Minnaert band, Proposition 6.4 (which combines Assumption 3 with the microscopic pole expansion of Proposition 2.1) implies that $\mathcal{H}_{\text{ext}}^\varepsilon(i\omega)$ has full row rank N and a uniformly controlled Moore–Penrose right inverse. We define $R_{I_M}^\varepsilon = \mathcal{F}^{-1} M_{(\mathcal{H}_{\text{ext}}^\varepsilon)^\dagger} \mathcal{F}$ via its frequency-domain multiplier:

$$\widehat{\lambda}^\varepsilon(i\omega) := \begin{cases} (\mathcal{H}_{\text{ext}}^\varepsilon(i\omega))^\dagger \widehat{q}^{\text{ideal}}(i\omega), & \omega \in I_M, \\ 0, & \omega \notin I_M. \end{cases}$$

By the exact algebraic identity $\mathcal{H}_{\text{ext}}^\varepsilon (\mathcal{H}_{\text{ext}}^\varepsilon)^\dagger = I_N$ on the row space, we obtain exact pointwise realization for the principal exterior-to-cluster map:

$$\mathcal{H}_{\text{ext}}^\varepsilon(i\omega) \widehat{\lambda}^\varepsilon(i\omega) = \widehat{q}^{\text{ideal}}(i\omega), \quad \omega \in I_M.$$

The discrepancy $\left\| \mathcal{F}^\varepsilon R_{I_M}^\varepsilon q^{\text{ideal}} - q^{\text{ideal}} \right\|_V \leq C_T \varepsilon^\beta$ between the causal mapping \mathcal{F}^ε and the stationary Fourier multiplier reduces strictly to temporal truncation errors. The initial rest conditions $q^{\text{ideal}}(0) = \dot{q}^{\text{ideal}}(0) = 0$ eliminate transient homogeneous solutions at $t = 0$. The residual spectral leakage from truncation at $t = T$ is then bounded by $\mathcal{O}(\varepsilon^\beta)$ via standard Paley–Wiener estimates.

We now estimate the physical control cost in the correct transducer norm. Since I_M is a bounded composite band, the Sobolev weights are uniformly bounded on its support. Hence, for $q \in V_{I_M} \subset H^1(0, T; \mathbb{R}^N)$,

$$\|R_{I_M}^\varepsilon q\|_{U_{\text{tr}}} \leq C(I_M) \sup_{\omega \in I_M} \|(\mathcal{H}_{\text{ext}}^\varepsilon(i\omega))^\dagger\|_2 \|q\|_V.$$

Here $C(I_M)$ depends only on the bounded operational frequency set and on the fixed time window, not on ε . This is precisely where the H^2 regularity of the physical transducer signals is reconciled with the H^1 cluster-source norm. As established in Proposition 6.4, the complete exterior-to-cluster map has a right inverse bounded by $\mathcal{O}(\eta_{\text{max}}/\varepsilon)$ on the composite Minnaert band. Thus

$$\|R_{I_M}^\varepsilon\|_{\mathcal{L}(V_{I_M}, U_{\text{tr}})} = \mathcal{O}\left(\frac{\eta_{\text{max}}}{\varepsilon}\right).$$

Because the physical acoustic radiation damping for every cluster intrinsically satisfies $\eta_\alpha = \mathcal{O}(\varepsilon)$, their maximum also satisfies $\eta_{\text{max}} = \mathcal{O}(\varepsilon)$. Therefore, the reciprocal scaling cancels, and the overall physical transducer cost remains strictly bounded:

$$\|R_{I_M}^\varepsilon\|_{\mathcal{L}(V_{I_M}, U_{\text{tr}})} = \mathcal{O}(1).$$

This completely bypasses the divergence obstacle associated with generic bands. ■

7 Energy Estimates and Proof of the Main Result

We are now in a position to analyze the two levels of our control problem and rigorously prove our main result, Theorem 2.5. We first construct the ideal actuator field p^{ideal} from the finite-dimensional tracking problem. The Minnaert-band hypothesis is then used only at the realization level, where the ideal source profile is generated by the finite-dimensional bubble system with uniformly bounded incident fields. Finally, we pass from the effective field $p^{\text{eff},\varepsilon}$ to the physical field p^ε by using the asymptotic error err_ε .

Let $I_M = \bigcup_{\alpha=1}^N I_\alpha(\varepsilon)$ be the composite Minnaert band and let $H_M = \text{span}\{\psi_k\}_{k=1}^{N_M}$ be the associated target spectral subspace. Let $T > 0$ and let $\mathbf{p}_r \in C^3([0, T]; \mathbb{R}^{N_M})$ be a prescribed reference trajectory vector satisfying the initial rest compatibility conditions

$$\mathbf{p}_r(0) = 0, \quad \dot{\mathbf{p}}_r(0) = 0.$$

We define the associated target spatial field $p_r^{I_M} \in C^3([0, T]; H_M)$ by $p_r^{I_M}(x, t) := \sum_{k=1}^{N_M} (\mathbf{p}_r(t))_k \psi_k(x)$. By Theorem 3.2, defining the ideal control vector

$$\mathbf{q}^{\text{ideal}}(t) := \frac{1}{c_0^2} L_M(\ddot{\mathbf{p}}_r(t) + \Lambda_M \mathbf{p}_r(t))$$

yields an ideal actuator field p^{ideal} such that the projection $P_{I_M} p^{\text{ideal}}(\cdot, t)$ exactly tracks the target field $p_r^{I_M}(\cdot, t)$ for all $t \in [0, T]$. This exact ideal tracking statement imposes no Minnaert-band restriction on the time profile of \mathbf{p}_r . For the subsequent physical realization estimate we assume that the induced profile $\mathbf{q}^{\text{ideal}}$ belongs to the composite band space V_{I_M} of Definition 4, or equivalently that its components admit finite-time extensions assigned to the separated cluster bands $I_\alpha(\varepsilon)$. This is the class for which Proposition 2.4 provides a uniformly bounded incident-field realization.

To bridge the physical H^1 control bound to the pointwise error dynamics of the wave equation, we establish the following uniform-in-time approximation.

Proposition 7.1 (Uniform-in-time approximation of the ideal sources). *Let $\mathbf{q}^{\text{ideal}} \in V_{I_M}$ and set the incident transducer fields as $\boldsymbol{\lambda}^\varepsilon := R_{I_M}^\varepsilon \mathbf{q}^{\text{ideal}}$. The effective bubble sources actually generated are then $\mathbf{q}^\varepsilon := \mathcal{T}^\varepsilon \boldsymbol{\lambda}^\varepsilon$. There exists $C_T > 0$ (independent of ε) such that*

$$\sup_{t \in [0, T]} \sum_{\alpha=1}^N \left| q_\alpha^\varepsilon(t) - q_\alpha^{\text{ideal}}(t) \right| \leq C_T \varepsilon^\beta \left\| \mathbf{q}^{\text{ideal}} \right\|_V. \quad (7.1)$$

Proof. By Proposition 6.6, we have

$$\left\| \mathbf{q}^\varepsilon - \mathbf{q}^{\text{ideal}} \right\|_V \leq C \varepsilon^\beta \left\| \mathbf{q}^{\text{ideal}} \right\|_V.$$

Since the source space is $V = H^1(0, T; \mathbb{R}^N)$, the estimate (7.1) follows immediately from the continuous Sobolev embedding $H^1(0, T) \hookrightarrow C^0([0, T])$ and the equivalence of norms on \mathbb{R}^N . \blacksquare

Let $p^{\text{eff},\varepsilon}$ be the effective pressure field in Ω satisfying (4.10). Define the effective tracking error:

$$e_{\text{eff}}^\varepsilon(x, t) := p^{\text{eff},\varepsilon}(x, t) - p^{\text{ideal}}(x, t).$$

Subtracting the ideal actuator model from the effective localized model gives, after projection onto H_M ,

$$\frac{1}{c_0^2} \partial_t^2 e_{\text{eff}}^\varepsilon - \Delta e_{\text{eff}}^\varepsilon = \sum_{\alpha=1}^N (q_\alpha^\varepsilon(t) - q_\alpha^{\text{ideal}}(t)) \delta_{y_\alpha} \quad \text{in the projected sense on } H_M, \quad (7.2)$$

with homogeneous Dirichlet boundary conditions and zero initial data. Notice that no residual force f^ε is introduced here; the asymptotic error of the physical bubbly field is kept separately as err_ε .

We project the effective error onto H_M . For $k \in \{1, \dots, N_M\}$, set

$$e_{k,\text{eff}}^\varepsilon(t) := \langle e_{\text{eff}}^\varepsilon(\cdot, t) | \psi_k \rangle.$$

Testing (7.2) against ψ_k gives the finite-dimensional forced oscillator vector system

$$\ddot{\mathbf{e}}_{M,\text{eff}}^\varepsilon(t) + \Lambda_M \mathbf{e}_{M,\text{eff}}^\varepsilon(t) = c_0^2 C_M (\mathbf{q}^\varepsilon(t) - \mathbf{q}^{\text{ideal}}(t)). \quad (7.3)$$

By (7.1), defining $\gamma_{\text{eff}} := \beta$, the forcing in the effective error system is bounded by

$$\sup_{t \in [0, T]} \left| c_0^2 C_M (\mathbf{q}^\varepsilon(t) - \mathbf{q}^{\text{ideal}}(t)) \right| \leq \tilde{C}_{T, M} \varepsilon^\beta. \quad (7.4)$$

We now define the modal energy of the band error vector $\mathbf{e}_{M,\text{eff}}^\varepsilon$:

$$E_M(t) := \frac{1}{2} \left(\left| \Lambda_M^{1/2} \mathbf{e}_{M,\text{eff}}^\varepsilon(t) \right|^2 + \left| \partial_t \mathbf{e}_{M,\text{eff}}^\varepsilon(t) \right|^2 \right).$$

Differentiating and substituting (7.3) gives:

$$E'_M(t) = \partial_t \mathbf{e}_{M,\text{eff}}^\varepsilon(t) \cdot \left(c_0^2 C_M (\mathbf{q}^\varepsilon(t) - \mathbf{q}^{\text{ideal}}(t)) \right).$$

Hence, by the Cauchy–Schwarz inequality and (7.4):

$$E'_M(t) \leq \sqrt{2E_M(t)} \tilde{C}_{T, M} \varepsilon^\beta.$$

Since the band initial data are perfectly matched, $\mathbf{e}_{M,\text{eff}}^\varepsilon(0) = \partial_t \mathbf{e}_{M,\text{eff}}^\varepsilon(0) = 0$, meaning $E_M(0) = 0$. Direct integration yields:

$$\sup_{t \in [0, T]} \sqrt{E_M(t)} \leq \tilde{C}_{T, M} T \varepsilon^\beta.$$

Finally, we translate the modal energy back to the spatial norms over Ω . Note that:

$$\|\nabla P_{I_M} e_{\text{eff}}^\varepsilon(\cdot, t)\|_{L^2(\Omega)}^2 = \frac{1}{c_0^2} \left| \Lambda_M^{1/2} \mathbf{e}_{M,\text{eff}}^\varepsilon(t) \right|^2, \quad \|P_{I_M} \partial_t e_{\text{eff}}^\varepsilon(\cdot, t)\|_{L^2(\Omega)} = \left| \partial_t \mathbf{e}_{M,\text{eff}}^\varepsilon(t) \right|.$$

Since H_M is finite-dimensional, $\|P_{I_M} e_{\text{eff}}^\varepsilon\|_{H^1}$ is strongly equivalent to $\|\nabla P_{I_M} e_{\text{eff}}^\varepsilon\|_{L^2}$. Thus, the uniform bounds on $\sqrt{E_M(t)}$ yield:

$$\sup_{t \in [0, T]} \left(\|P_{I_M} e_{\text{eff}}^\varepsilon(\cdot, t)\|_{H^1(\Omega)} + \|P_{I_M} \partial_t e_{\text{eff}}^\varepsilon(\cdot, t)\|_{L^2(\Omega)} \right) \leq C_T \varepsilon^\beta. \quad (7.5)$$

Recalling that $e_{\text{eff}}^\varepsilon = p^{\text{eff}, \varepsilon} - p^{\text{ideal}}$ and using $P_{I_M} p^{\text{ideal}} \equiv p_r^{I_M}$ gives the effective tracking estimate. The physical field satisfies $p^\varepsilon = p^{\text{eff}, \varepsilon} + \text{err}_\varepsilon$. Because the projection P_{I_M} maps into a finite-dimensional space of smooth functions H_M , all norms on H_M are equivalent, and the vanishing volume of the bubbles $|D| = \mathcal{O}(\varepsilon^3)$ ensures that $\|P_{I_M} \text{err}_\varepsilon\|_{H^1(\Omega)} \leq C \|P_{I_M} \text{err}_\varepsilon\|_{H^1(\Omega \setminus \bar{D})}$ for sufficiently small ε . Hence, by the projected asymptotic estimate (4.14),

$$\begin{aligned} & \sup_{t \in [0, T]} \left(\|P_{I_M} (p^\varepsilon - p_r^{I_M})(\cdot, t)\|_{H^1(\Omega)} + \|P_{I_M} \partial_t (p^\varepsilon - p_r^{I_M})(\cdot, t)\|_{L^2(\Omega)} \right) \\ & \leq C_T \varepsilon^\beta + C_T \varepsilon^\mu \leq C_T \varepsilon^\gamma, \quad \gamma := \min\{\beta, \mu\}. \end{aligned}$$

This recovers the tracking bound stated in (2.38).

Finally, by the explicit definition of the applied transducer fields $\lambda^\varepsilon := R_{I_M}^\varepsilon q^{\text{ideal}}$ and the uniform operator bound from Proposition 6.6, the physical control cost is strictly governed by:

$$\|\lambda^\varepsilon\|_{U_{\text{tr}}} \leq \|R_{I_M}^\varepsilon\|_{\mathcal{L}(V_{I_M}, U_{\text{tr}})} \|q^{\text{ideal}}\|_V \leq \kappa_M \|q^{\text{ideal}}\|_V,$$

which completes the proof of Theorem 2.5. ■

References

- [1] L. V. Ahlfors, *Complex Analysis: An Introduction to the Theory of Analytic Functions of One Complex Variable* (3rd ed.). McGraw-Hill, 1979.
- [2] H. Ammari; D-P. Challa; A-P. Choudhury; M. Sini, The equivalent media generated by bubbles of high contrasts: volumetric metamaterials and metasurfaces. *Multiscale Model. Simul.* 18 (2020), no. 1, 240-293.
- [3] H. Ammari; D-P. Challa; A-P. Choudhury; M. Sini, The point-interaction approximation for the fields generated by contrasted bubbles at arbitrary fixed frequencies. *J. Differential Equations* 267 (2019), no. 4, 2104-2191.
- [4] H. Ammari, B. Fitzpatrick, D. Gontier, H. Lee and H. Zhang, Minnaert resonances for acoustic waves in bubbly media, *Ann. Inst. H. Poincaré C Anal. Non Linéaire* 7 (2018), 1975-1998.
- [5] H. Ammari and H. Zhang, Effective medium theory for acoustic waves in bubbly fluids near Minnaert resonant frequency, *SIAM J. Math. Anal.* 49 (2017), 3252-3276.
- [6] C. Bardos, G. Lebeau, and J. Rauch, Sharp sufficient conditions for the observation, control, and stabilization of waves from the boundary, *SIAM Journal on Control and Optimization*, 30 (1992), pp. 1024–1065.
- [7] R. E. Caflisch, M. J. Miksis, G. C. Papanicolaou, and L. Ting, Effective equations for wave propagation in bubbly liquids, *J. Fluid Mech.* 153 (1985), 259–273.
- [8] A. Dabrowski, A. Ghandriche and M. Sini. Mathematical analysis of the acoustic imaging modality using bubbles as contrast agents at nearly resonating frequencies, *Inverse Probl. Imaging* 15 (2021), 555-597.
- [9] J. K. Hale and S. M. Verduyn Lunel, *Introduction to Functional Differential Equations*, Applied Mathematical Sciences 99, Springer, New York, 1993.
- [10] R. A. Horn and C. R. Johnson, *Matrix Analysis* (2nd ed.). Cambridge: Cambridge University Press, 2012.
- [11] T. Kato, *Perturbation Theory for Linear Operators*, Classics in Mathematics, Springer-Verlag Berlin Heidelberg, 1995.
- [12] S. G. Krantz and H. R. Parks, *A Primer of Real Analytic Functions*, 2nd ed. Boston, MA: Birkhäuser, 2002.
- [13] K. Kunisch, S. S. Rodrigues and D. Walter, Stabilizability for nonautonomous linear parabolic equations with actuators as distributions, *ESAIM Control Optim. Calc. Var.* 30 (2024), Paper No. 43.
- [14] J.-L. Lions, *Exact Controllability, Stabilization and Perturbations of Distributed Systems*, Masson, Paris, and SIAM, Philadelphia, 1988.
- [15] L. Li and M. Sini, High-contrast transmission and Fabry–Pérot resonances, *arXiv:2510.19096*.
- [16] W. Michiels and S.-I. Niculescu, *Stability and Stabilization of Time-Delay Systems*, SIAM, 2007.
- [17] L. Miller, *Controllability cost of conservative systems: Resolvent condition and transmutation*, *J. Funct. Anal.* 218 (2005), 425–444.
- [18] A. Mukherjee and M. Sini, Time-dependent acoustic waves generated by multiple resonant bubbles: application to acoustic cavitation, *J. Evol. Equ.* 24 (2024), 90–155.

- [19] A. Mukherjee and M. Sini, Dispersive effective model in the time-domain for acoustic waves propagating in bubbly media, *SIAM J. Appl. Math.* 85 (2025), 2508–2542.
- [20] A. Mukherjee, S. S. Rodrigues and M. Sini, Feedback Stabilization and Tracking for Heat Equations Using Thermo-Plasmonic Nanoparticles as Actuators, preprint, 2026, arXiv:2602.14581.
- [21] E. M. Stein and R. Shakarchi, *Complex Analysis*. Princeton University Press, 2003.
- [22] M. Tucsnak and G. Weiss, *Observation and Control for Operator Semigroups*, Birkhäuser, Basel, 2009.
- [23] M. Tucsnak, and G. Weiss, *From exact observability to identification of singular sources*. *Math. Control Signals Systems* 27 (2015), no. 1, 1–21.
- [24] E. Zuazua, Controllability and observability of partial differential equations: some results and open problems, in *Handbook of Differential Equations: Evolutionary Equations*, Vol. 3, Elsevier, 2007, 527–621.